

6102120

Gulf Science and Technology Company
Pittsburgh, Pennsylvania

SEISMIC EXPLORATION OF A PORPHYRY
COPPER DEPOSIT - BUTTE VALLEY, NEVADA

by

James E. Fix

Exploration Department

Technical Memorandum No. 4206TG641

File No. 4206FROO

July, 1976

**UNIVERSITY OF UTAH
RESEARCH INSTITUTE
EARTH SCIENCE LAB.**

Table of Contents

LIST OF FIGURES.....	i
LIST OF TABLES.....	iii
ABSTRACT.....	iv
I. INTRODUCTION.....	1
A. Objective.....	1
B. Location and Brief History.....	1
C. Seismic Techniques.....	2
D. Organization of Report.....	2
II. GEOLOGY SUMMARY.....	4
A. Butte Valley Prospect.....	4
B. Porphyry Copper Model.....	5
III. TOPOGRAPHY AND SEISMIC LINES.....	8
IV. REFRACTION STUDY.....	11
A. Objective.....	11
B. Data.....	11
C. Method.....	19
D. Results.....	20
1. Linear Refractions.....	20
2. Fan Refractions.....	28
E. Interpretation.....	32
V. REFLECTION STUDY.....	41
A. Objective.....	42
B. Data.....	42
C. Results.....	43
D. Interpretation.....	43
E. Interpretation Summary.....	53
VI. MAGNETIC STUDY.....	55
VII. CONCLUSIONS.....	59
VIII. RECOMMENDATIONS.....	60
REFERENCES.....	62
ACKNOWLEDGEMENTS.....	63

List of Figures

Figure 1.	Location Map Butte Valley Prospect, White Pine County, Nevada.....	2
Figure 2.	Concentric alteration - mineralization zones in a typical porphyry deposit (a) schematic drawing of alteration zones showing exposure levels of several porphyry copper deposits (b) schematic drawing of mineralization zones (c) schematic drawing of the occurrence of sulfides (after Lowell and Guilbert, 1970).....	7
Figure 3.	Generalized diagrammatic section summarizing geometry of alteration in several porphyry copper deposits in the Robinson District, Nevada (after James, 1976).....	9
Figure 4.*	Aerial photograph of Butte Valley, Nevada, Prospect with overprint of seismic line and station location	
Figure 5.	Travel time curve, Line 1, linear refraction.....	12
Figure 6.	Travel time curve, Line 2, linear refraction.....	14
Figure 7.	Travel time curve, Line 3, linear refraction.....	15
Figure 8.	Travel time curve, Line 4, linear refraction.....	16
Figure 9.	Travel time points, Lines 1, 2, 3, fan refraction.....	17
Figure 10.	Travel time points, Line 4, fan refraction.....	18
Figure 11.	Line 1 inversion model and drill hole lithology.....	21
Figure 12.	Line 2 inversion model and drill hole lithology.....	24
Figure 13.	Line 3 inversion model and drill hole lithology.....	25
Figure 14.	Line 4 inversion model and drill hole lithology.....	27
Figure 15.	Fan refraction average velocities, Line 1, 2, and 3.....	29
Figure 16.	Fan refraction average velocities, Line 4.....	30
Figure 17.	Surface projection of fan refraction rays with average velocities ≥ 2896 m/s (9500 ft/s).....	31
Figure 18.	Isopach two layers of Quarternary alluvium, Butte Valley Prospect, Nevada.....	36
Figure 19.	Isopach Ely Limestone and Chainman Shale, Butte Valley Prospect, Nevada.....	37
Figure 20.	Isopach Diamond Peak Quartzite, Butte Valley Prospect, Nevada.....	39
Figure 21.	Elevation of top of 6294 m/s layer 6 (qm, Pej, or PeSK).....	40
Figure 22.*	Line 3, Butte Valley, Nevada, Seismic Section	
Figure 23.*	Line 4, Butte Valley, Nevada, Seismic Section	
Figure 24.*	Line 5, Butte Valley, Nevada, Seismic Section	
Figure 25.	Line 3, Butte Valley, Nevada, Interpreted Seismic Section.....	45
Figure 26.	Line 4, Butte Valley, Nevada, Interpreted Seismic Section.....	48

*These figures are in the attached folder.

Figure 27. Line 5, Butte Valley, Nevada, Interpreted Seismic Section.....	51
Figure 28.* Total magnetic field reduced to the pole, elevation 2286 m (7500 ft.), Butte Valley, Nevada	
Figure 29. Approximate shape of magnetic model superimposed on seismic section line 5	57
Figure 30. Total magnetic field, model and observed, line 5.....	58

*These figures are in the attached folder.

List of Tables

TABLE 1. Geologic Symbols.....	22
TABLE 2. Model Velocity, Model Layer, and Lithology Interpretations.....	33
TABLE 3. Interface Depths and Refractor Velocities on Intersecting Lines.....	34

Abstract

A seismic survey was conducted at a porphyry copper prospect in Butte Valley, Nevada, where 16 drill holes provided subsurface control. The data set includes 4 lines of linear and fan refraction data and 3 lines of CDP reflection data. The primary objective of defining the geologic structure was achieved with the delineation of structural features not previously detected with the drill holes or with geologic, gravity, magnetic, and vector IP exploration. The inversion of the linear refraction data identified interfaces among six layers at depths down to 760 m. A westward dipping structure with major faults and grabbens is outlined. Average velocities and interface depths tied closely between intersecting lines. The deepest layer had an igneous rock velocity of 6300 m/s and dipped from depths of 150 m in the east to 670 m in the west. Based on the fan refraction data, the most probable location for the monzonite stock is about 610 m ESE of drill hole BV9. The interpretation of the CDP data reveals a complicated subsurface with folding and parallel faults in conjugate shear patterns resulting from an upward force. In places, en echelon faults create repeated sections, previously identified only as thickened sections. Surface traces of three faults are identified in the aerial photograph and seismic sections. The faulting cuts all lithologic units including a still developing fanglomerate indicating continued tectonic activity that will help maintain channels for water flow and secondary enrichment. Extensive high grade metamorphism has altered sedimentary beds that produce excellent reflections in the central valley so that the reflections lose their distinctive characteristics. Lithology can be identified and followed in the vicinity of the drill holes, but interpretations across the many faults are speculative. A seismic section is used to define the geometry for a 2D model that

atches the magnetic total field. It is recommended that: (1) reflection surveys be considered as a prospect evaluation technique to determine structure for optimization of an exploratory drilling program; (2) concurrent refraction surveys be used for a first generalization of lithologic units; and (3) that methods of improving lithologic detection in areas of complex faulting and folding be investigated.

I. INTRODUCTION

A. Objective

The objective of the survey in Butte Valley, White Pine County, Nevada, is to demonstrate the capabilities of seismic methods applied to the exploration of a porphyry copper prospect. The immediate objective is to delineate the geologic structure to aid in the interpretation of the relationship of the quartz monzonite intrusive to the altered host rocks and thereby provide information useful for designing a program of exploratory holes, or in the case of Butte Valley of selecting locations for additional exploratory holes.

To demonstrate the success of this survey, it is necessary to have adequate subsurface control. The Butte Valley Prospect has sixteen exploratory holes that provide considerable information in the immediate vicinity of the survey. This prospect was selected in conjunction with Kennecott Exploration, Inc., (Kennecott) because of these subsurface data and other information known to Kennecott.

As an early seismic experiment at a porphyry copper prospect, the first requirement was to collect good data with essentially conventional seismic methods. It was not considered appropriate for this survey to jeopardize data quality to experiment with potential cost saving methods of source type, sensors, recording instrumentation, or field procedures.

B. Location and Brief History

The Butte Valley Prospect is located in T22N, R61E, White Pine County, Nevada, about 80 road km north and west of Ely (see Fig. 1). About 13 km west of Ely is the Robinson Mining District where large-scale copper production has been continuous since 1908 in underground and open pit mines. The Butte Valley

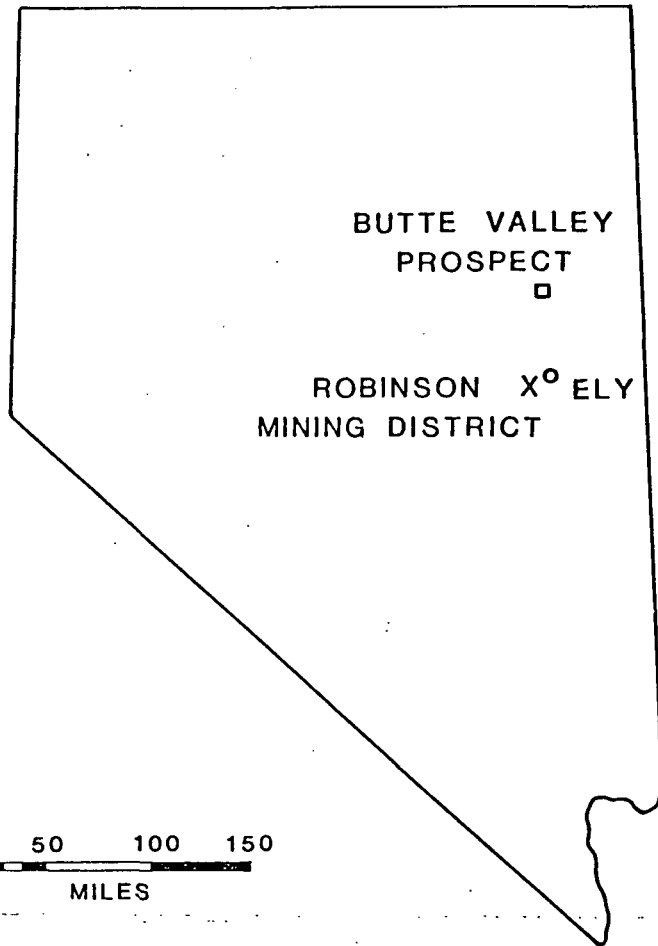


FIGURE 1. LOCATION MAP BUTTE VALLEY PROSPECT,
WHITE PINE COUNTY, NEVADA

property is on the west flank of the Cherry Creek Range and about 20 km west-southwest of the Cherry Creek Mining District.

The location was originally noticed as an anomaly on aeromagnetic data taken by Gulf with a high-altitude survey of eastern Nevada. In the early 1960's New Jersey Zinc and Newmont explored the anomaly with ground magnetometer and IP surveys and drilled a 305 m (1,000 ft.) hole without finding the magnetic source. During 1964, Cyprus Mines became interested and drilled a 700 m (2,300 ft.) hole (BV-1) through a 35.7 m (117 ft.), 0.77% Cu enriched chalcocite zone into mineralized porphyry. After five additional holes failed to produce a better delineation of an ore body, a joint venture agreement was made with Bear Creek Mining Company in 1967. Since then, Bear Creek has completed nine holes and is drilling the tenth to fulfill annual assay requirements. The best hole to date has been the first Cyprus hole. Since Bear Creek's participation, Kennecott has conducted two aerial surveys and one ground survey of total magnetic field, one magnetic gradiometer survey, and vector IP surveys along nine lines. (Frangos and Wright, 1972).

This joint effort between Kennecott and Gulf was initiated by Dr. T. R. Hopkins, President, GR&DC and Dr. Milton Stern, Vice President - Exploration, Kennecott Copper Corporation, in October, 1974.

C. Seismic Techniques

Three seismic techniques were used during this survey: common-depth-point (CDP) reflection seismology, linear refraction seismology, and fan refraction seismology.

D. Organization of Report

The geologic setting of Butte Valley and of representative porphyry copper deposits are outlined in Section II. The geometry of the seismic lines is described in Section III. The refraction study is presented in Section IV with

the reflection study in Section V. A preliminary magnetic study is reported in Section VI. Conclusions and Recommendations are presented in Sections VII and VIII.

II. GEOLOGY SUMMARY

A. Butte Valley Prospect

The Butte Valley prospect is a porphyry copper-type sulfide system of major proportions, with an already drill-indicated mineralized area of at least two square miles. A large magnetic skarn is present which may contain economic quantities of ore-grade mineralization. Conditions are right for the formation and preservation of a supergene enrichment blanket. Primary mineralization of economic grade may also be present. (Frangos and Wright, 1972).

The mineralization is associated with an intrusive which varies between quartz monzonite and quartz rhyolite porphyry which has formed sills within the typically complex, overthrust eastern Nevada stratigraphy of the Mississippian Chainman Shale Formation near the contact with Pennsylvanian Ely Limestone. The sulfide system is covered by a Tertiary fanglomerate, a gravity slide block of Ely, Diamond Peak, and Chainman Formations, and Quaternary and Recent gravels. Depth to mineralized bedrock varies from about 550 m (1,800 ft.) (drill holes BV-1, 4, and 7) to about 760 m (2,500 ft.) (BV10 and 11). A complicated and poorly understood geologic history has resulted in a complex structural interpretation by Miller (1971). (Frangos and Wright, 1972).

Miller (1971) describes the chronology of the major geologic events that took place at the prospect. These events are:

- Pre-intrusive thrust faulting
- Intrusive activity
- Post-intrusive/pre-oxidation faulting
- Oxidation and enrichment
- Post oxidation faulting
- Erosion

Volcanic activity

Deposition of tertiary fanglomerate

Regional westward tilting and subsequent gravity slide block

Deposition of quarternary and recent alluvium

Geology of the adjacent Cherry Creek Range has been mapped by Fritz (1968).

The slopes of the Cherry Creek Range rise to the east of the prospect with beds dipping 20 to 50 degrees to the west. These steep dips are associated with the tectonic activity that resulted in the gravity slide block that overlays the mineralized zone. The regional extent of gravity slide blocks in this part of Nevada is discussed in a recent article by Armstrong (1972). Other recent papers on the geology of the region discuss the Permian-Triassic boundary (Collinson, et al., 1976) and the stratigraphy immediately to the north of the prospect (Marcantel, 1975).

B. Porphyry Copper Model

To aid in a definition of the structural problem addressed by this seismic study, this section summarizes the geologic structure and alteration-mineralization zones of a porphyry copper ore body model. The features of this model can serve as a reference for interpretation of the seismic data. The literature on porphyry copper deposits is extensive and no attempt has been made to present a thorough review here.

Lowell and Guilbert (1970) outline a typical sequence of events in the deposition of a porphyry deposit. An initial deep porphyry copper melt, unsaturated with water at 1 to 3 per cent is intruded as a stock at depths less than about 1350 m (4,500 ft.) Rupture by faulting causes a sudden, even explosive, loss of water and results in supercooling of the silicate melt. Faults and brecciated zones possibly occur during this sudden event. The supercooling produces crystallization with a porphyritic-aphanitic texture and the upward progress of the now dry melt is halted. Volatiles released by the quenching migrate outward through crackle, stockwork, and brecciated zones in the cooler margins.

Augmented by diffusion effects, alteration and mineralization occur in response to temperatures from near magmatic at the center of the stock to relatively cool temperatures in the wall rocks. Subsequent extensive argillic alteration shown by most porphyry copper deposits is probably due to a superimposed circulating geothermal hot-spring system fed mainly by meteoric and connate waters.

The resulting structure is a series of concentric alteration-mineralization zones schematically illustrated in Figure 2 from Lowell and Guilbert (1970). The alteration zones (Fig. 2a) grade from an outer propylitic zone through argillic and phyllic zones to an inner potassic zone. The exposure levels of several porphyry copper deposits in relation to the model are shown in the figure also. The mineralization zones are shown in Fig. 2b. The peripheral zone does not contain commercial grade copper or molybdenum. Typically, 70% of the ore is in the igneous intrusive rock and 30% in the altered country rock in the pyrite shell. The occurrence of sulfides (Fig. 2c) is in decreasing size from veins outside the peripheral zone, veinlets within the peripheral zone, predominantly veinlets with some dissemination in the pyrite shell, predominantly disseminated with some veinlets in the ore shell, to dissemination and microveinlets in the low grade core.

The Robinson Mining District, west of Ely has yielded ore exceeding \$1.3 billion in total value that has been produced from five open pits and numerous underground mines. The geologic setting as described by James (1976) is very similar to the geology of the Butte Valley Prospect. The Ely Limestone and underlying Chainman shale formations were involved in a thrust fault of regional extent. Major folding along north-south axes accompanied or followed the thrusting. In Cretaceous time, monzonitic magma intruded along the thrust and fracture zones and spread upward among overlying irregular blocks of Ely Limestone. High angle normal faulting followed magma consolidation and mineralization. Normal faults with small dis-

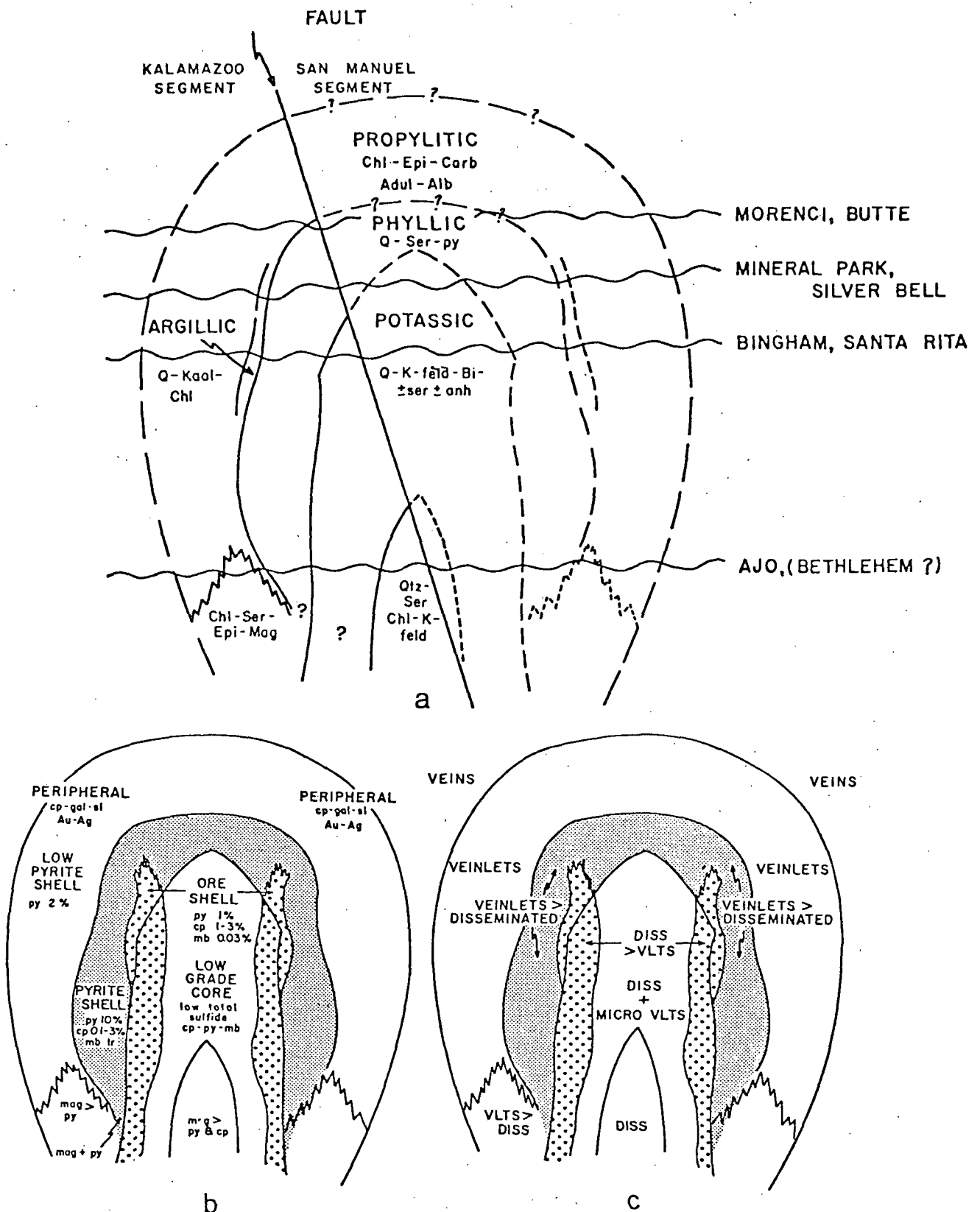


FIGURE 2. CONCENTRIC ALTERATION-MINERALIZATION ZONES IN A TYPICAL PORPHYRY DEPOSIT (A) SCHEMATIC DRAWING OF ALTERATION ZONES SHOWING EXPOSURE LEVELS OF SEVERAL PORPHYRY COPPER DEPOSITS (B) SCHEMATIC DRAWING OF MINERALIZATION ZONES (C) SCHEMATIC DRAWING OF THE OCCURENCE OF SULFIDES (AFTER LOWELL AND GUILBERT, 1970)

placement occur every few feet in many pit faces, yielding very complex local structure. Faults with large displacements can be detected by the offset of identifiable rock units or alteration types and usually by the presence of thick gouge zones. There are three alteration zones in the limestone: tactite, silica-pyrite, and peripheral and two alteration zones in the porphyry: biotite-orthoclase and quartz-sericite. Figure 3 is a generalized diagrammatic section from James (1976) summarizing the geometry of these alteration zones. The tactite and biotite-orthoclase zones are the primary ore locations.

III. TOPOGRAPHY AND SEISMIC LINES

The surface topography over most of the seismic survey area is divided into two general regions separated by a major fault. This fault has about a 7 m topographic relief and was interpreted only as a lake terrace by Kennecott (Miller, 1971, Welsh, personal communication, 1976). During the data collection, the present writer recognized this topographic feature as a fault and extended two of the seismic lines to the south and east to provide additional subsurface data for a better definition of its extent. The surface expression of this fault is clearly visible in the aerial photograph in Fig. 4* as a broad open U trending from the south in a northeasterly direction then changing to north-westerly. To the west of the fault, the terrain is flat; the vegetation is grass or low sage brush; and the soil is very fine particle clayey sand. To the east of the fault, the terrain is gently sloping to the foothills of the Cherry Creek Range; the vegetation is medium height sage brush; and the soil is sandy with erosion pebbles no larger than 1/8 in. dimension.

The seismic lines and station locations are overprinted on the aerial photograph. The station numbering is as follows: first digit for line number, dash, one or two digit sequential number on 137.2 m (450 ft.) spacing, dash, followed by blank, 1, 2, or 3 for intermediate stations on 34.3 m (112.5 ft.) spacing. The

*Figure 4 is in the attached folder.

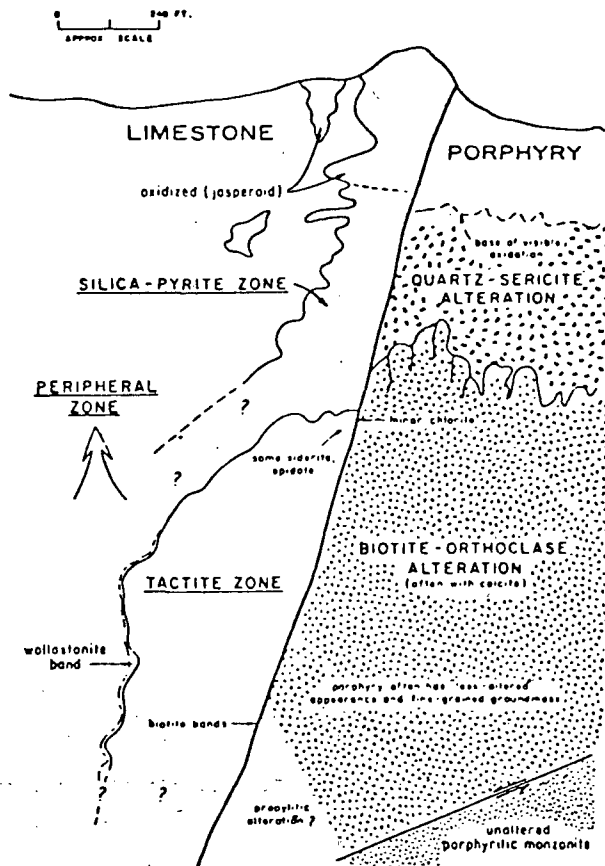


FIG. 3 GENERALIZED DIAGRAMMATIC SECTION SUMMARIZING GEOMETRY OF ALTERATION IN SEVERAL PORPHYRY COPPER DEPOSITS IN THE ROBINSON DISTRICT, NEVADA. (AFTER JAMES, 1976)

approximate positions of the exploratory drill holes are also shown as BV (number). Lines 1, 2 and 5 were terminated short of the apex of the triangle because of the steeply rising Ely Limestone outcrop to the east. The lines were laid out with drill hole BV9 at the center of the triangle because the drill data indicated it was the center of the quartz monzonite stock. Seismic data were taken as follows:

Linear refraction:

Lines: 1, 2, 3, 4

Station Spacing: 137.2 m (450 ft.)

Number of shots: 5 on lines 1, 2, 3; 7 on line 4

Fan refraction:

Line 1 from shot point 2-47

Line 2 from shot point 1-1

Line 3 from shot point 5-4

Line 4 from shot points 2-74, 1-20, and 1-12

Common-depth point reflection:

Lines: 3, 4, 5

Station spacing: 34.3 m (112.5 ft.)

Geophone arrays: 18 geophones, 8 Hz,
3.3 m (11 ft.) spacing,
57 m (187 ft.) length

End-on shots on 68.6 m (225 ft.) spacing

Shot offset: line 3 - 34.3 m (112.5 ft.)
line 4 and 5 - 68.6 m (225 ft.)

Shot charge: 0.227 kg (1/2 lb.) primer

Fold of CDP: 6

Recording filters: low cut - 16 Hz, 24dB/octave
high cut-out

Sampling interval: 1 ms

Dates of field data recording: 9/25/75 - 10/18/75

Two seismic lines recorded by Gulf in 1955 are also located in Figure 4. The trace of these lines is clearly identifiable today. The aerial photograph and drill hole locations were supplied by Kennecott. Since the 1955 lines do not appear on the photograph, it must predate 1955.

IV. REFRACTION STUDY

The refraction study is an independent seismic study described in this section. The objectives are given in Section A; the data are presented in Section B; the method of inverting the linear refraction data is discussed in Section C; the results are presented in Section D and are interpreted in Section E.

A. Objective

The objective of the linear refraction study is to evaluate the capabilities of using the less costly technique of seismic refraction profiles to delineate the structure in a complicated geologic setting such as a porphyry copper deposit. This study provides an independent definition of the structure.

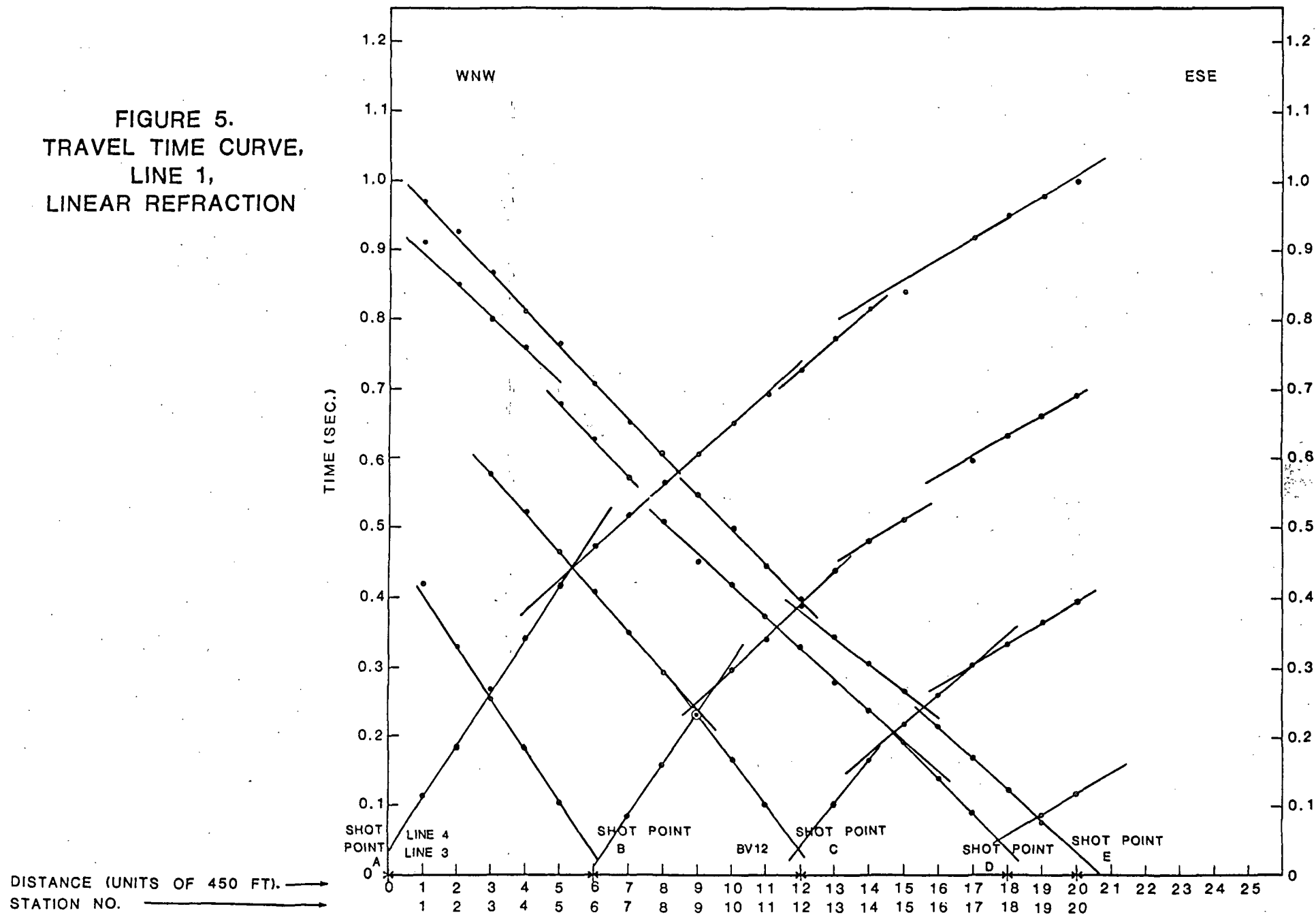
The objective of the fan refraction study is to outline the limits of the quartz monzonite intrusion by shorter travel times through the faster igneous rock as compared to the metamorphosed sediments adjacent to it. This concept has been successfully applied in the Gulf Coast region to delineate salt domes.

B. Data

The data were recorded at a sampling interval of 1 ms from 4.5 Hz vertical geophones at 137.2 m (450 ft.) spacing. The recordings were played back at an enlarged amplitude so that the time of the first break could be reliably determined with ease. Second arrivals were looked for but only a few could be identified. Only first arrivals were used in the inversions.

The travel time curve for line 1 is plotted in Figure 5. Several constant velocity segments are defined by the data. Evidence for faulting is also clear at several places by offsets in parallel line segments. A block upthrown to the east

FIGURE 5.
TRAVEL TIME CURVE,
LINE 1,
LINEAR REFRACTION



is indicated for shot point A by refractions received at stations 11 and 12. Blocks down thrown to the west are indicated for shot D by refractions received at stations 4 and 5 and at stations 7 and 8, and a block downthrown to the east is indicated for shot B for refractions received at stations 15 and 17. A shallow high velocity layer is indicated for shot E by the refraction recorded at stations 13, 14, and 15.

The travel time curve for line 2 is plotted in Figure 6. Considerably more complexity is indicated for the structure under line 2.

The travel time curve for line 3 is plotted in Figure 7. Line 3 was originally intended as an "off-the-anomaly" line. The results show that it is still within the disturbed area but it has the least complicated geologic structure. The refractions from shot point A (station 3-70) are used as a reference for the fan refractions.

The travel time curve for line 4 is plotted in Figure 8.

The travel times are plotted against surface distance in Figure 9 for the fan refraction shots into the three sides of the triangle, lines 1, 2 and 3. The station numbers are given beside the data points. A segment of the linear refraction profile from shot point A (station 3-70) for line 3 is also plotted. All but three of the travel times are seen to be earlier for the fan shots than for the "nominal" shot along line 3. Significant differences can be seen in the travel times between the two ends of all three lines.

The fan refraction travel times for three shots into line 4 are plotted against surface distance in Figure 10. All of the travel times are earlier than for the "nominal" shot along line 3. Significant differences can be seen in the travel times between the two ends of line 4 with high velocities at the southeast end.

7T

FIGURE 6.
TRAVEL TIME CURVE,
LINE 2,
LINEAR REFRACTION

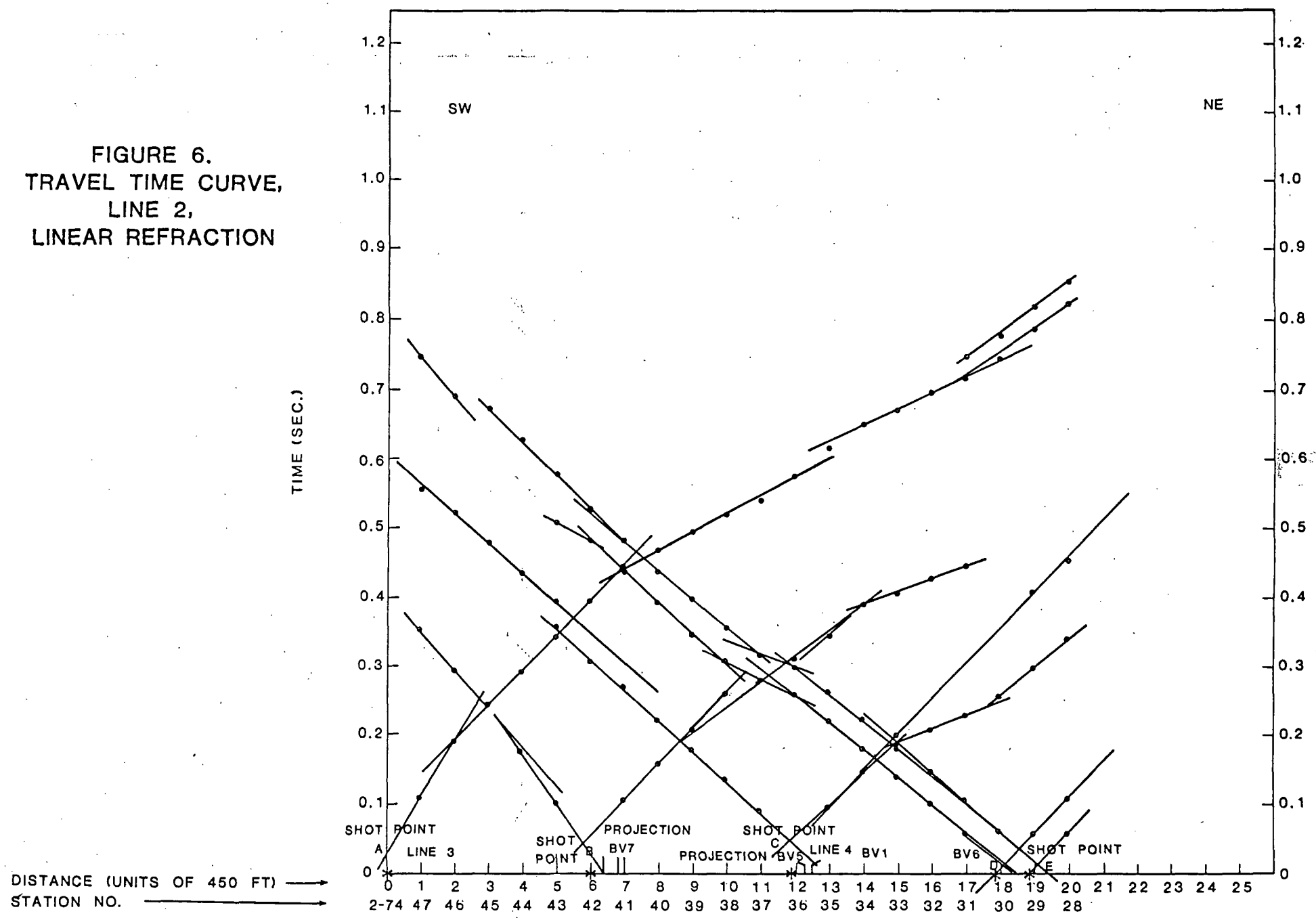


FIGURE 7.
TRAVEL TIME CURVE,
LINE 3,
LINEAR REFRACTION

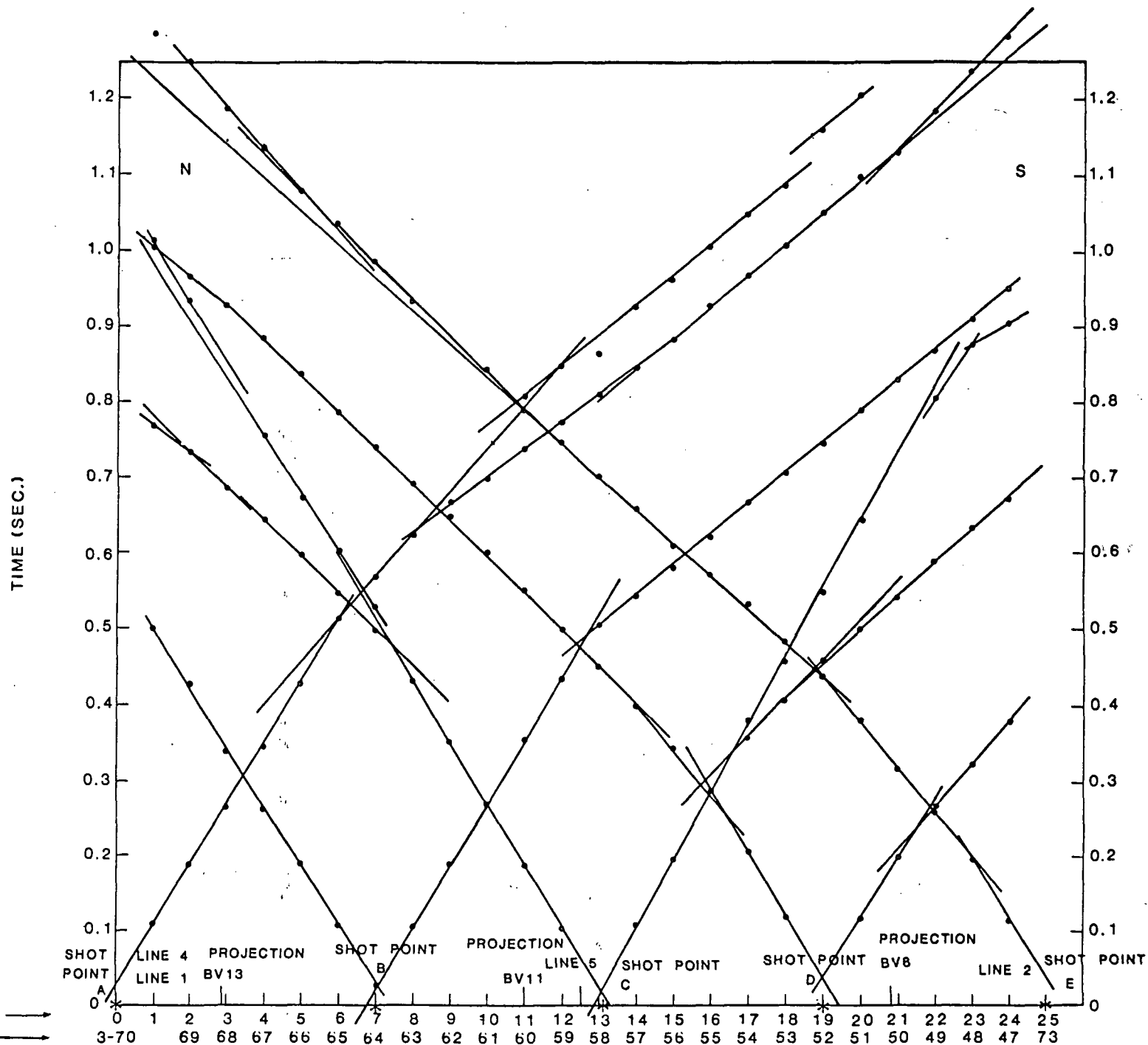
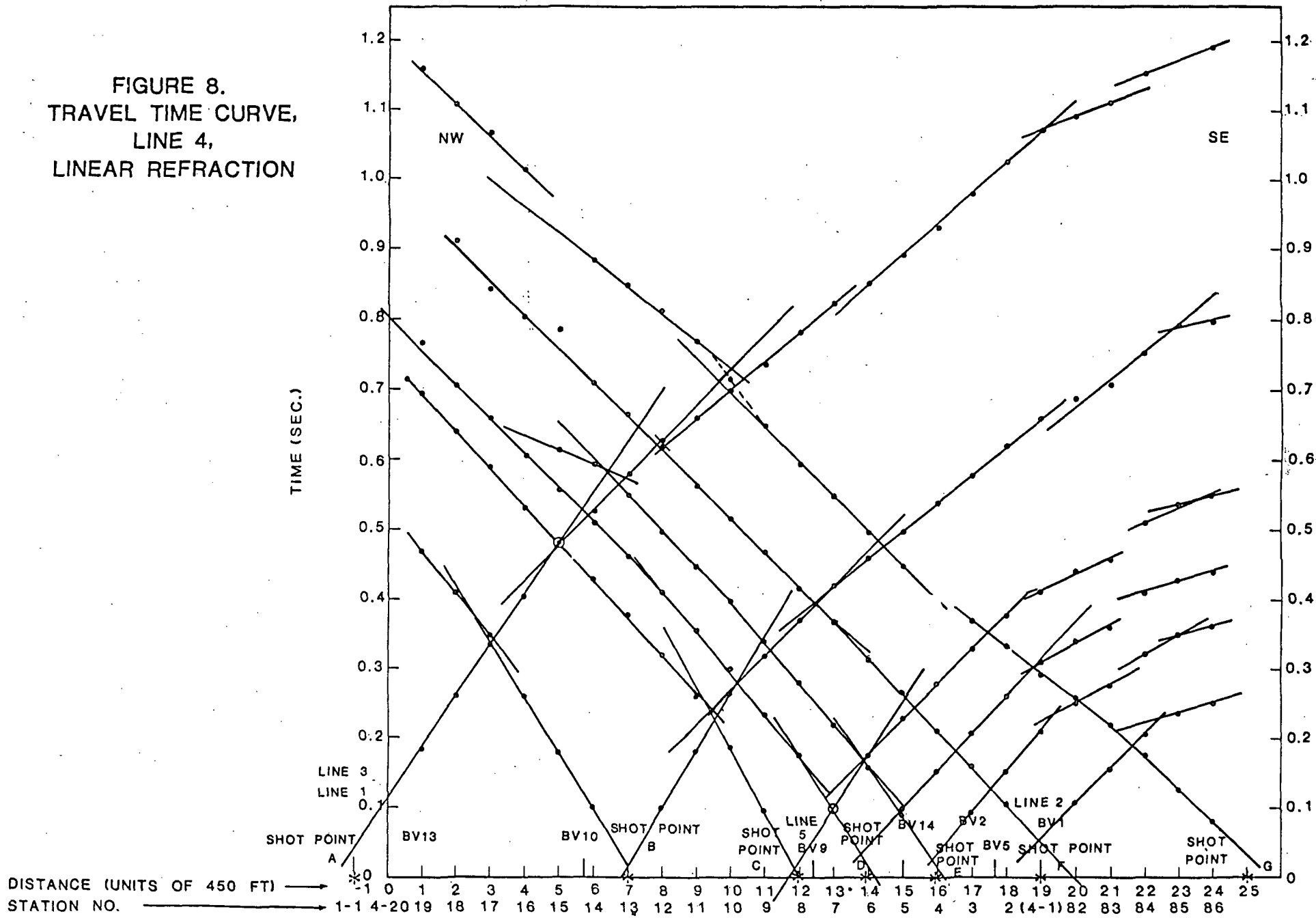
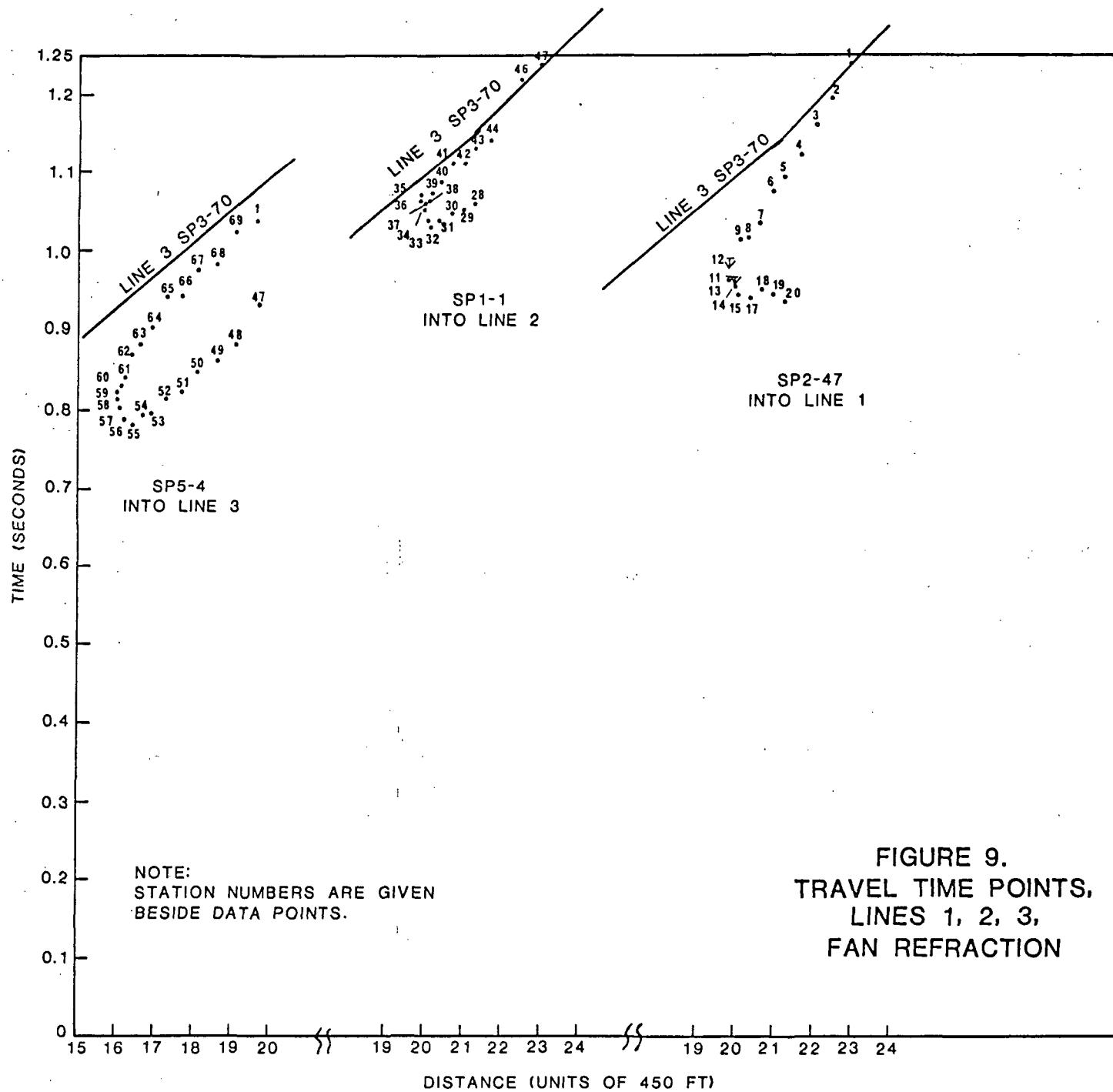


FIGURE 8.
TRAVEL TIME CURVE,
LINE 4,
LINEAR REFRACTION





18

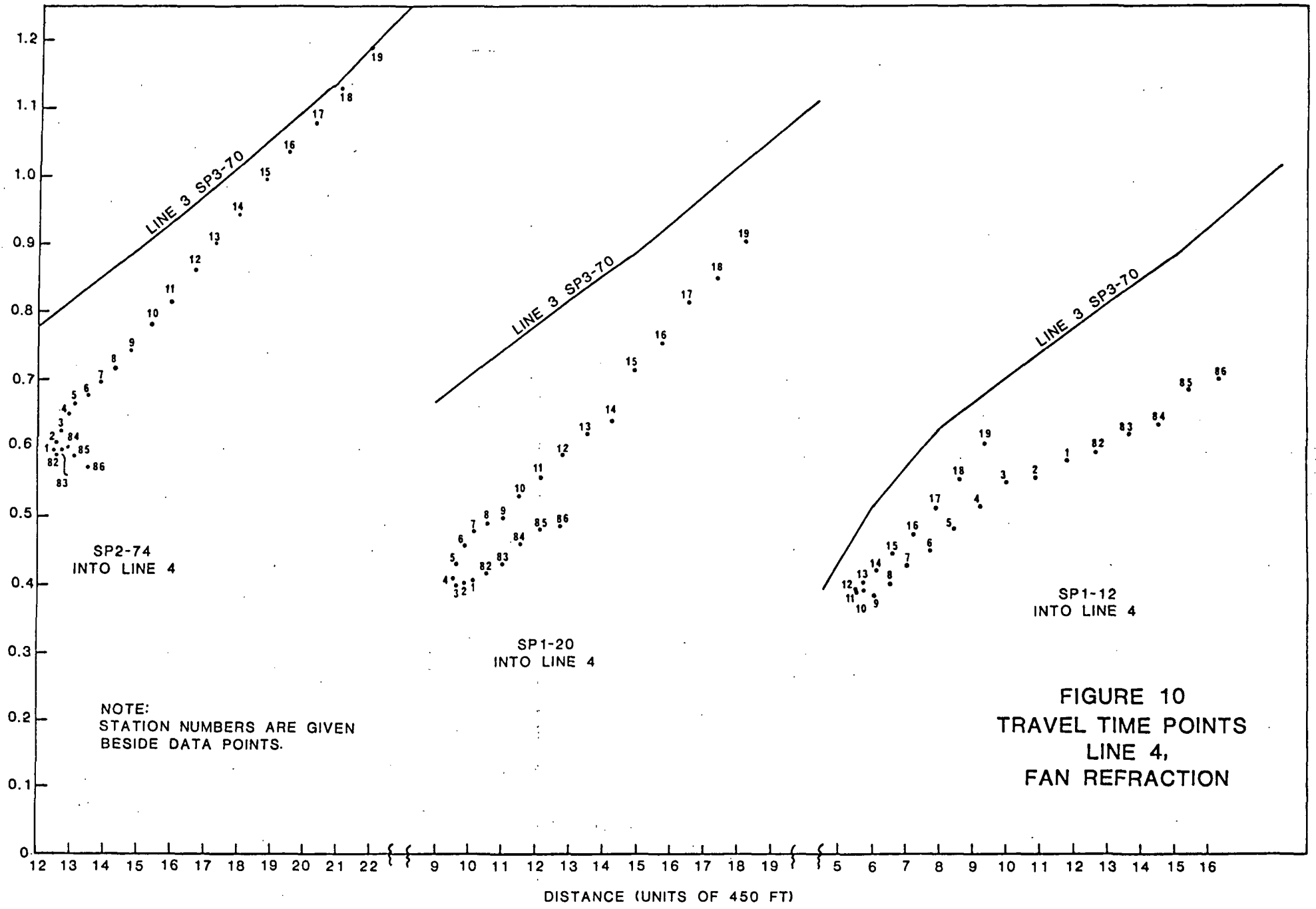


FIGURE 10
TRAVEL TIME POINTS
LINE 4,
FAN REFRACTION

C. Method

The linear refraction data were inverted to produce models of the structure along the four lines. A computer program developed at the Bureau of Mines (Scott, et al., 1970) was used for the inversion. The program, as implemented at Gulf Science and Technology Company (GS&TC) will accommodate input travel times from 48 geophones, 7 shot points, and 5 layers. For the input, the analyst associates an arrival time with the layer that is the deepest layer penetrated by the refraction ray. The program calculates the velocity of the various layers, performs a ray tracing calculation from each shot point to each receiver, establishes the penetration point of each ray through its deepest interface, iterates four times through the ray tracing calculations for a least squares fit of all the data, fits a polynomial through the ray traced penetration points for each interface and outputs the data on a line printer with plots of the travel time curves and inversion models. The program has a provision for the analyst to input layer velocities to override the calculated velocities.

In the inversions reported in the results in Section IV.D., the solutions are the pure result of the data and have not been selected on any other criteria. The velocity of layer one was hand calculated using the updip and downdip velocities. This velocity was input to the program. The velocities of the other three or four layers were calculated by the program. Because of the complicated geology and the large dips, there was a possibility of misassociating arrival times and layers. Arrival times were first assigned to the five layers based on apparent velocities. Solutions were obtained and ray penetration points through the interfaces that appeared to be mislocated from the majority of the data were adjusted. In all of the final solutions, the program used all of the data available to it and all of the penetration points were reasonably scattered about their respective interfaces.

D. Results

Any refraction solution is an average in velocity and in layer interface depth. Since the solution is an average along the line, the refraction method has a resolution much coarser than the reflection seismic method.

1. Linear Refractions

The four-layered inversion solution model and the solution velocities for line 1 linear refraction data is illustrated in Figure 11. The lithology of drill hole BV12 as tabulated by Kennecott is overprinted on the inversion model. The lithology tabulated by Kennecott is based mostly on drill cuttings. Cores were taken at horizons with altered mineralogy. The lithology used throughout this report is that summarized by Welsh (1976). Welsh states "the quality of the rotary cuttings in all holes is poor and the lithologies and interpretations vary ... between geologists." The geological symbols used throughout the report are given in Table 1. The vertical exaggeration in these and the following similar figures is 1.54:1. The inversion model is a perfect fit to the interface at the bottom of the Ely Limestone and top of the Chainman Shale and to the top of the quartz monzonite. The fit to the quartz monzonite is fortuitous at this depth especially with the steep dip. The Tertiary fanglomerate is expected to be a low velocity layer and should not have a refraction arrival. The discrepancy between the alluvium and Ely Limestone interface at BV12 is unexplained and is accepted as a difference between the inversion and the drill hole lithology. The Kennecott geologists report that not many cuttings were retained from the alluvium. There is a reflector within the alluvium seen in the reflection sections that is not identified in the Kennecott lithology. There is a possibility that at BV12 the interface that is assigned to the alluvium-Ely Limestone contact is actually the shallower layer within the alluvium, but

LINE 1 INVERSION MODEL AND DRILL HOLE LITHOLOGY

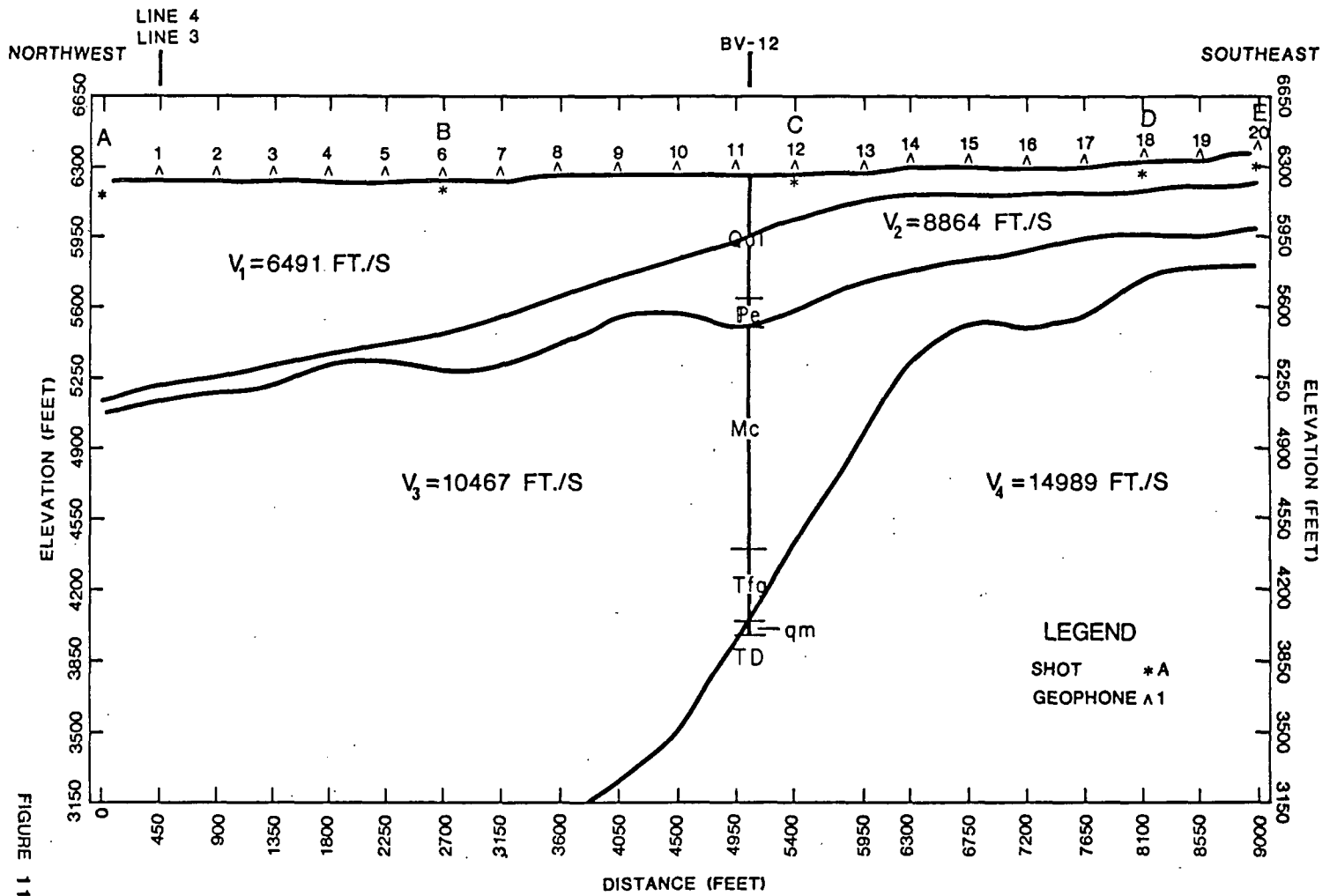


FIGURE 11

TABLE 1

Geologic Symbols

Unknown Age:

Ftc	fanglomerate - tuff, carbonates
Fics	fanglomerate - limestone, chert, sandstone
Fs	fanglomerate - sandstone
Ft	fanglomerate - tuffaceous matrix, sandstone, limestone
L	latite

Quaternary:

Qal	alluvium
-----	----------

Tertiary:

qr	quartz rhyolite porphyry
qm	quartz monzonite
Tfg	fanglomerate

Pennsylvanian:

Pe	Ely Limestone
Pej	Ely Jasperoid
PeSK	Ely Skarn

Mississippian:

Mc	Chainman Shale Formation
McDP	Diamond Peak Quartzite member of Chainman Shale Formation
McHF	Chainman Shale Hornfels
Mj	Joana Limestone
MjJ	Joana Jasperoid
MjSK	Joana Skarn

Devonian:

Dg	Guilmette Formation
Dp	Pilot Shale
DpSK	Pilot Skarn

this possibility is discounted. The Ely Limestone is hard and is difficult to drill so the driller's identification of the top of this unit must be accepted. Structurally, there are steep dips down to the west. The steeply dipping interface at the top of layer 4 is interpreted as a major fault.

The five layered inversion solution model and solution velocities for line 2 linear refraction data is illustrated in Figure 12. The lithology of drill holes BV1, 5, 6, and 7 as tabulated by Kennecott is overprinted on the inversion model. The lithology between the drill holes has been connected with smooth lines by the present author in a manner similar to the illustrations of Miller (1971). The two layers within the alluvium are delineated by the inversion model but not by the drill hole lithology. The top of the Ely Limestone is a good fit at BV6, but is off at the other three drill holes, especially BV5 which is 135 m (450 ft.) north of line 2. The top of the Diamond Peak Quartzite has the proper dip, but the inversion interface is shallower than the actual contact. The top of the fifth layer is significantly shallower than the next interface indicated by the lithology.

The four-layered inversion model and solution velocities for line 3 are illustrated in Figure 13. The Kennecott interpreted lithology is overprinted on the inversion model. This line was expected to be away from the major disturbances. The structure is perpendicular to dip and is much flatter and less complicated than the other profiles. However, a grabben is indicated between stations 68 and 63. The two layers within the alluvium are present. The top of the Ely Limestone is accurately located at BV11 but is shallow at the projection of BV8. The top of the fourth layer coincides with the quartz monzonite at BV11 but does not agree with any lithologic interface at BV8. The 3212.2 m/s (10,539 ft/s) velocity is slow for the quartz monzonite. This velocity suggests that the fourth interface is probably the top of the Diamond Peak Quartzite.

LINE 2 INVERSION MODEL AND DRILL HOLE LITHOLOGY

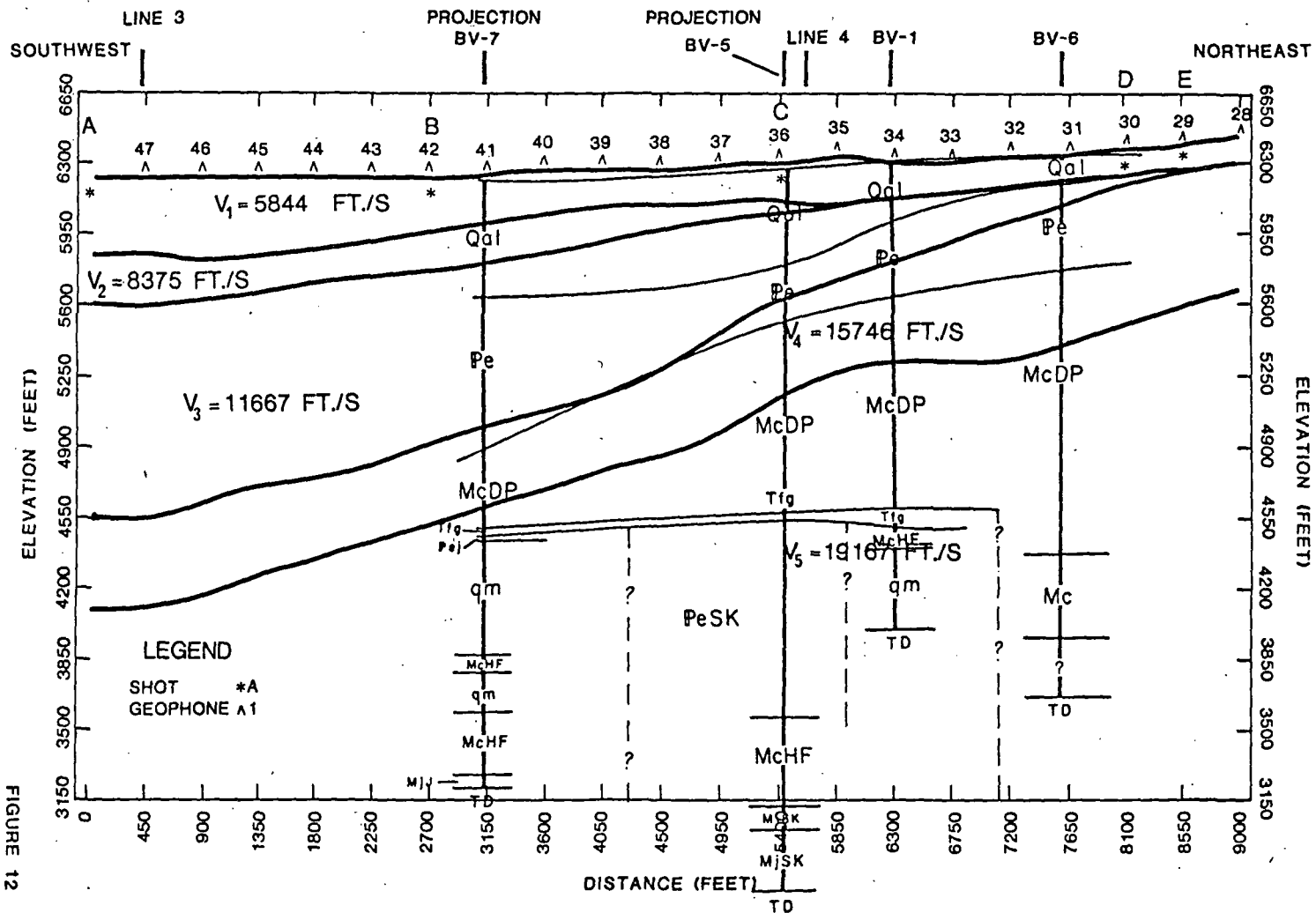


FIGURE 12

LINE 3 INVERSION MODEL AND DRILL HOLE LITHOLOGY

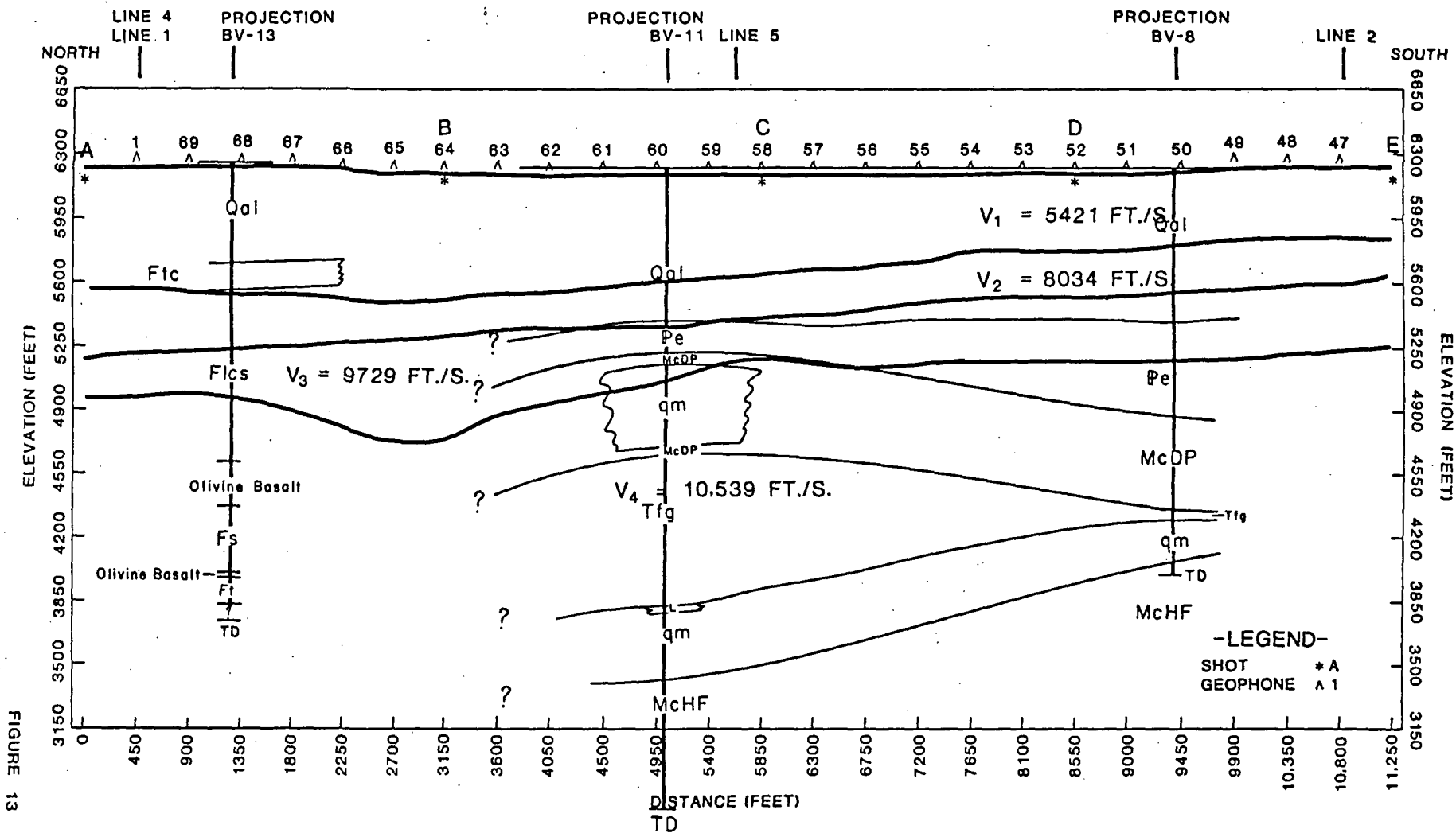


FIGURE 13

The five layered inversion model and solution velocities for line 4 are illustrated in Figure 14. The Kennecott interpreted lithology is overprinted in the figure. The two layers within the alluvium are defined by the inversion; however, the second layer has a faster velocity than in the other three lines. This difference will be discussed later. The top of the Ely Limestone is defined relatively well and the grabben at BV5 was detected. The surfaces dipping to the northwest between stations 7 and 14 on the interface between layers 3 and 4 and between stations 32 and 4 on the interface between layers 4 and 5 are interpreted as faults. The top of layer 4 is interpreted to be the top of the Diamond Peak Quartzite. Good fits to this interface are achieved at BV14, BV5, and BV1. The Chainman Shale at BV10 probably has a velocity similar to the Ely Limestone and was not separated at BV10. The top of the fifth layer is a representative fit to the depth of the top of the Tertiary fanglomerate along the gravity slide block. The velocity for this layer is representative of igneous rocks and not a fanglomerate--even a well cemented fanglomerate. The fanglomerate should be a low velocity layer that would introduce a time delay, that would not have observable refractions, and that would result in a deeper inversion interface for the quartz monzonite. Yet, the inversion models in all four lines fit the fanglomerate better than the quartz monzonite. This must be accepted as an error in the solution at these nominal 610 m (2,000 ft.) depths. The rise of the top of layer 5 to the southeast does not correspond with the lithology in BV5 and BV1. To provide a better tie to the inversion solution for line 2, the fault along the interface between layers 3 and 4 is extended from station 7 to station 5. The second layer is then interpreted as alluvium to the northwest of this extended fault and Ely Limestone to the southeast. The high average velocity for this layer is interpreted as an average between the two lithologies.

LINE 4 INVERSION MODEL AND DRILL HOLE LITHOLOGY

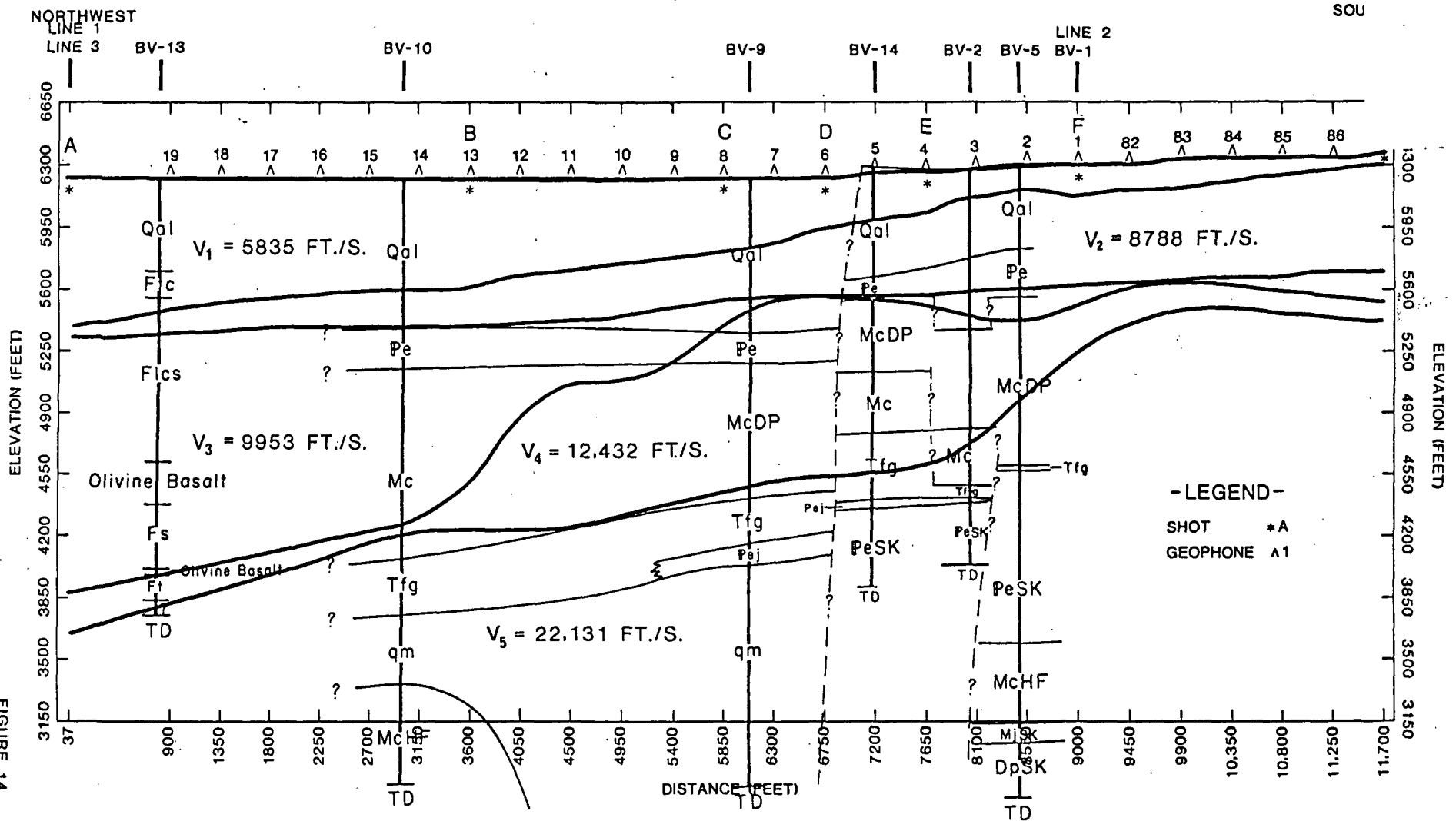


FIGURE 14

2. Fan Refractions

The fan refractions were shot from the corners of the triangle (or as close as possible) and were recorded along the opposite side. If there was a homogeneous halfspace with a constant velocity, the stations at the minimum distance would receive the signal first with uniform time delays on both sides of the minimum distance. If there was a cylindrical high velocity intrusion in the center of the triangle, as envisioned by the Kennecott interpretation originally supplied to Gulf, the refraction rays passing through the high velocity zone would arrive earlier than in the uniform velocity case. The dimensions of the intrusion could then be estimated from the early arrivals. A non-symmetrical travel time set was observed (Figures 9 and 10).

If all the stations were an equal distance from the shot point, time differences could be used directly. Since the stations in this study were at different distances, average surface velocity is used for comparison. The average surface velocity is defined as the surface distance from shot to receiver divided by travel time. This average velocity is a gross parameter that is a non-linear result of layer thicknesses, velocities, and dips. The average velocities for lines 1, 2 and 3 are plotted in Figure 15 and for the three shots into Line 4 are plotted in Figure 16. The large increase in velocity to the east is emphasized in these figures.

The surface projection of rays with average velocities of 2895.6 m/s (9,500 ft/s) and greater are plotted in Figure 17. This velocity range was selected arbitrarily. The subtended angle is shaded at the shotpoints for identification of the paths included. Within the included angles, the number of overlapping ray segments is listed. The heaviest concentration of high velocities is seen to be in the southeast center of the triangle where four

FIGURE 15.
 FAN REFRACTION
 AVERAGE VELOCITIES,
 LINE 1, 2, AND 3

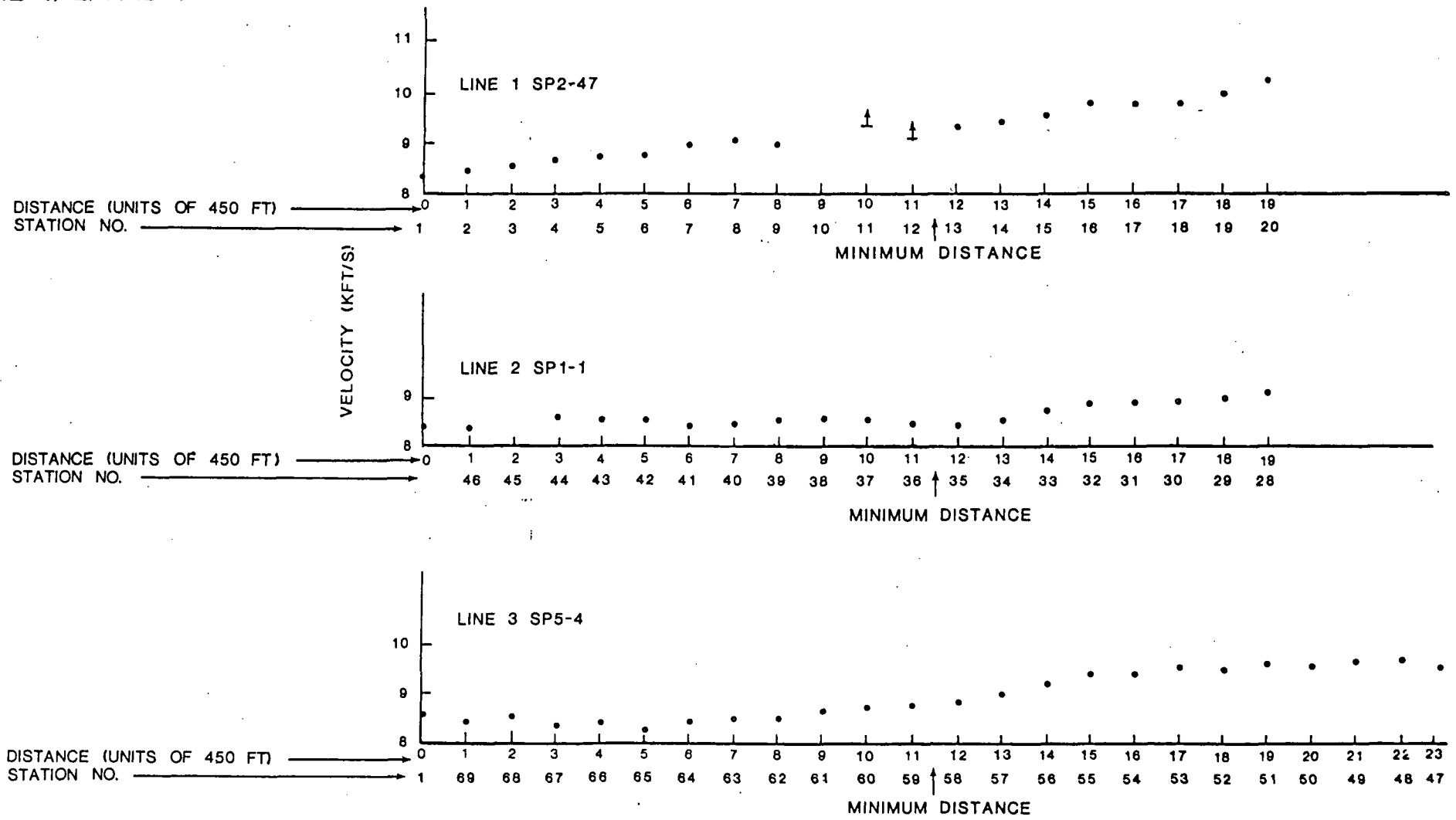
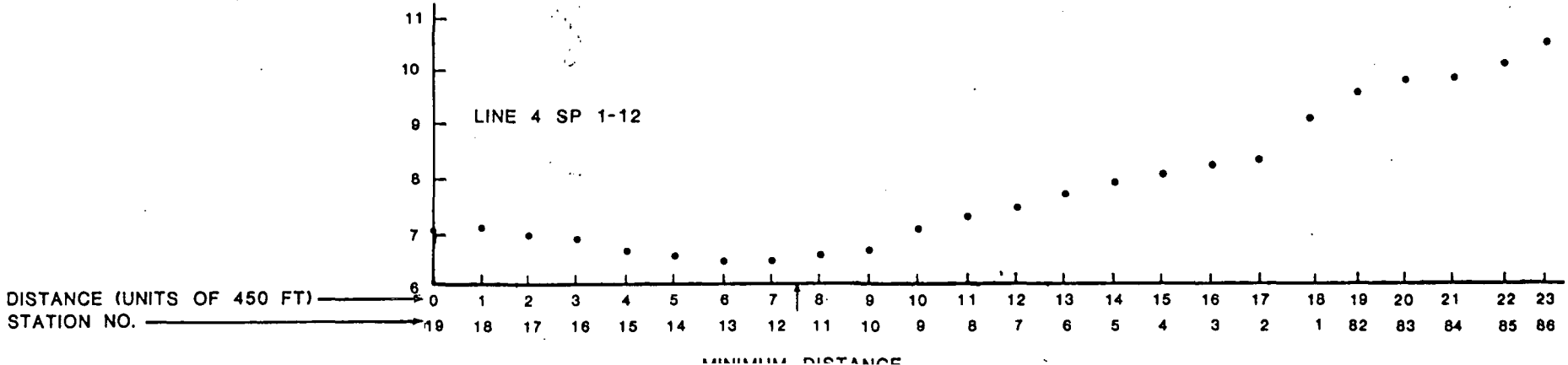
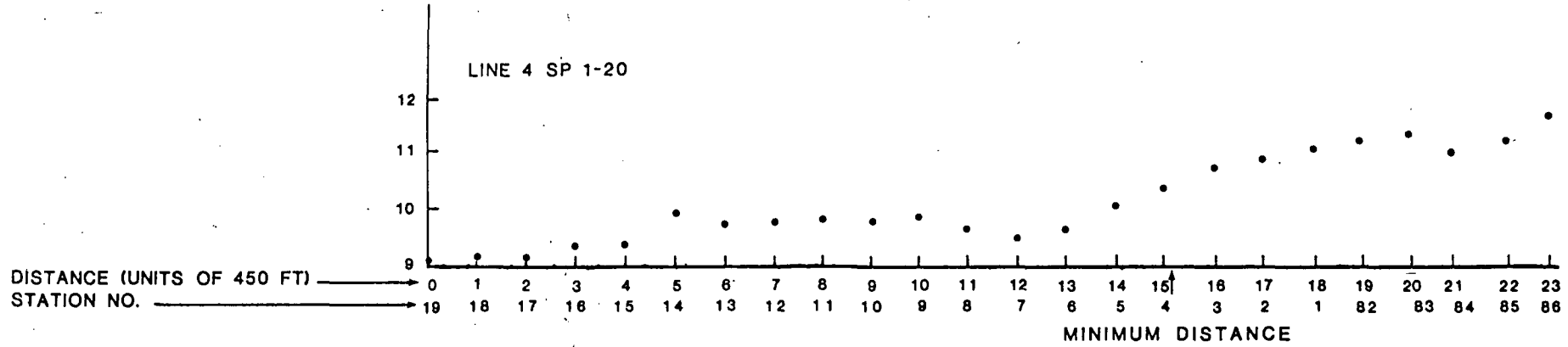
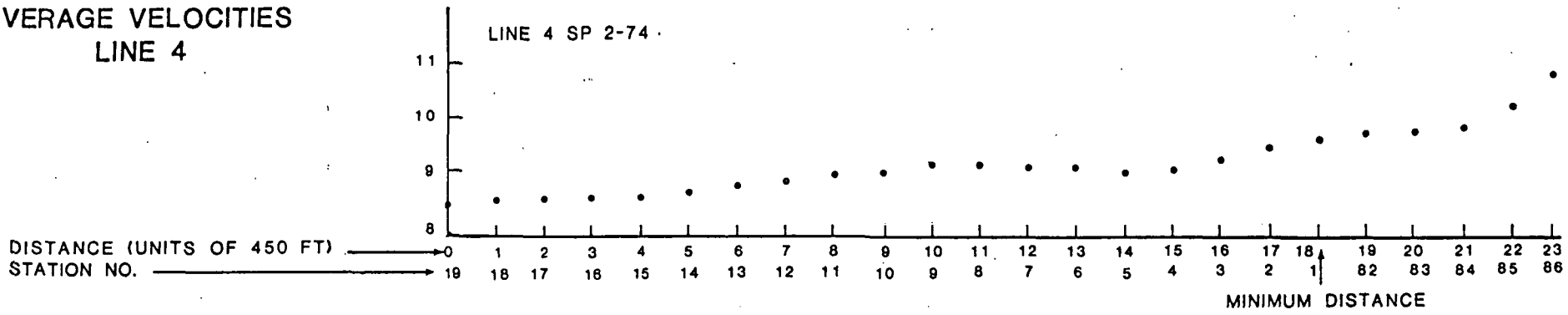


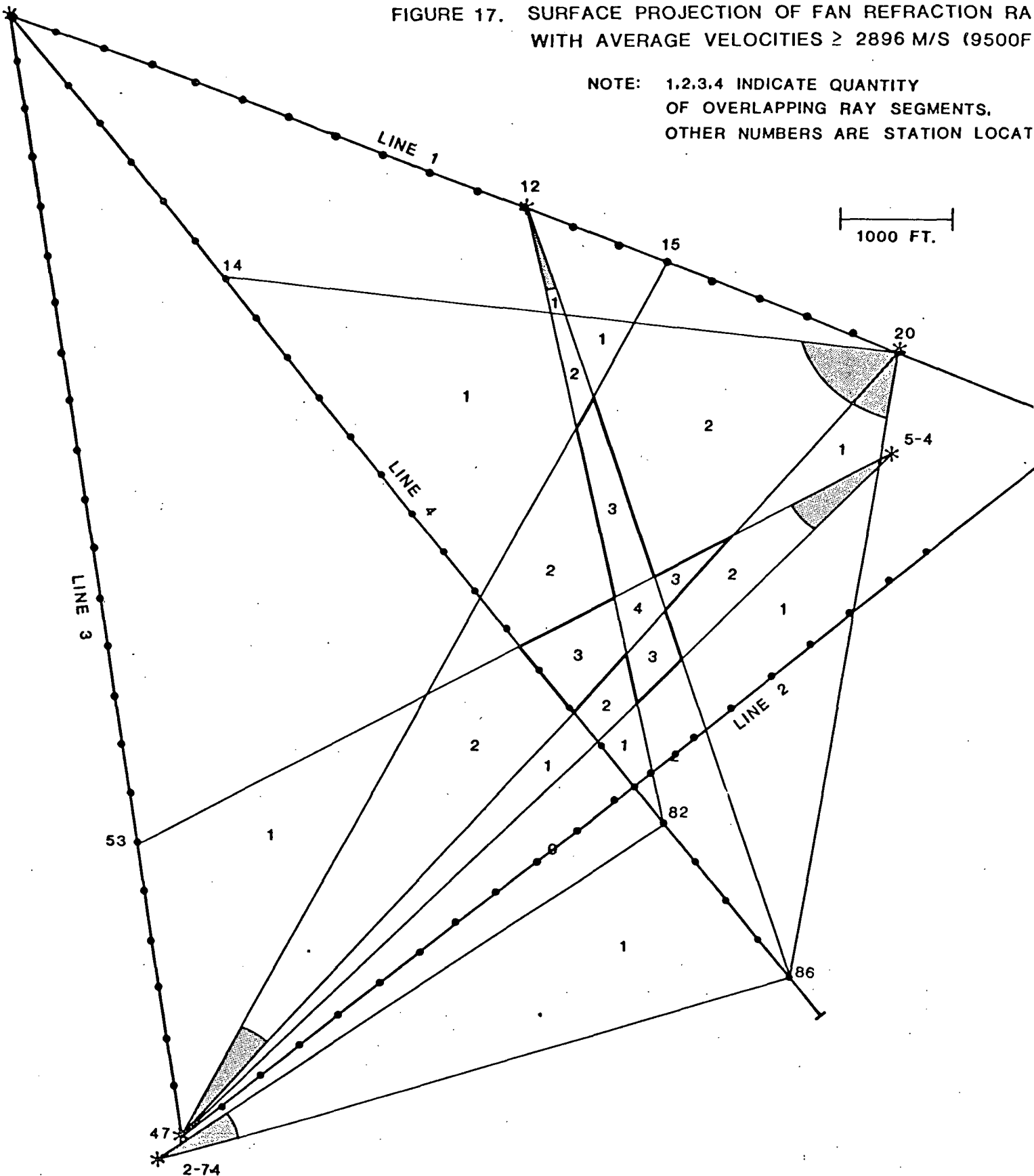
FIGURE 16
 FAN REFRACTION
 AVERAGE VELOCITIES
 LINE 4



30

FIGURE 17. SURFACE PROJECTION OF FAN REFRACTION RA
WITH AVERAGE VELOCITIES ≥ 2896 M/S (9500F)

NOTE: 1,2,3,4 INDICATE QUANTITY
OF OVERLAPPING RAY SEGMENTS.
OTHER NUMBERS ARE STATION LOCAT



sets of ray segments overlap. The high velocities from shot point 2-74 to line 4 stations 82 to 86 were along paths not traversed by other rays.

E. Interpretation

The primary interpretation result from the refraction survey is an independent determination of the structural features in the area. The results are considered very good. Velocities have been determined and layer surfaces have been outlined for four or five layers at depths down to 760 m (2,500 ft.). Since the refraction method is based on average velocities and a smooth curve fit to interfaces, this method results in a coarse definition of the general structure.

The solution models indicate a steeply dipping subsurface with layers rising to the east and southeast. Two graben structures are outlined and several major faults can be interpreted from the inversions. Portions of the prospect have significantly higher velocities or higher velocities at shallower depths than the general area. These higher velocities are on the upthrown side of normal faults on lines 4 and 1. Velocities representative of igneous rocks represent the lower layer on lines 2 and 4. The agreement with the drill hole lithology is satisfactory with many solution interfaces being at the exact depths. In other locations, the fits are not as good. Two layers are distinct within the Quaternary alluvium. In general, the overall structural solution is compatible to the structural interpretation from the drill data.

The ties between the four lines are exceptional. The velocities of the several layers provide a guide for layer comparison. The results are interpreted in terms of six layers. The solution velocities are given in Table 2 with the interpreted layer, interface, and lithology. The interface depths and the refraction velocities on intersecting lines are given in Table 3. For four independent solutions, these solutions show the capability of the refraction

TABLE 2

Model Velocity, Model Layer, and Lithology Interpretations

layer	1	2	3	4	5	6
interface	1	2	3	4	5	6
lithology	Qal	Qal	Pe	Mc	McDP	qm or PeJ or PeSK
<u>line</u>	Velocity (m/s) (Velocity (ft/s))					
1	--	1978 (6491)	2702 (8864)	3190 (10467)	4569 (14989)	--
2	1791 (5844)	2553 (8375)	3556 (11667)	--	4799 (15746)	5842 (19167)
3	1652 (5421)	2449 (8034)	2965 (9727)	3212 (10539)	--	--
4	1779 (5835)	2679 (8788)	3034 (9953)	--	3789 (12430)	6746 (22131)

TABLE 3

Interface Depths and Refractor Velocities on Intersecting Lines

Interface Number	Elevations (m) Velocity (m/s)		(Elevations (ft) - Velocity (ft/s))	
	Line			
	1	2	3	4
3	1584.5 - 2702 (5198.5 - 8864)		1587.0 - 2965 (5206.8 - 9727)	
4	1563.1 - 3190 (5128.4 - 10467)		1515.3 - 3212 (4971.4 - 10539)	
2		1779.6 - 2553 (5338.6 - 8375)	1781.4 - 2449 (5844.6 - 8034)	
3		1703.2 - 3556 (5588.0 - 11667)	1709.6 - 2965 (5608.8 - 9727)	
2		1860.1 - 2553 (6102.8 - 8375)		1869.6 - 2679 (6133.8 - 8788)
3		1851.8 - 3556 (6075.3 - 11667)		1869.6 - 3034 (6133.8 - 9953)
5		1728.1 - 4799 (5669.6 - 15746)		1672.8 - 3789 (5488.1 - 12432)
6		1589.8 - 5842 (5216.0 - 19167)		1594.7 - 6746 (5232.0 - 22131)

method. Of the eighteen velocities in Table 2 only three might be assigned to other layers if velocity were the only criteria. The line 1 velocities of 1978 and 2702 m/s could be associated with the two alluvium layers rather than the second alluvium layer and the Ely Limestone. The line 2 velocity of 3556 m/s fits layer 4, the Chainman Shale, better than the Ely Limestone. However, the Chainman Shale does not appear in the lithology of this line. These three velocities have been associated with their respective layers based on the lithology and the depths of intersecting lines.

To aid in the interpretation of the structure as determined from the refraction study, three isopachs and the gross surface contour of the top of the 6294 m/s (20,650 ft/s) layer 6 have been plotted.

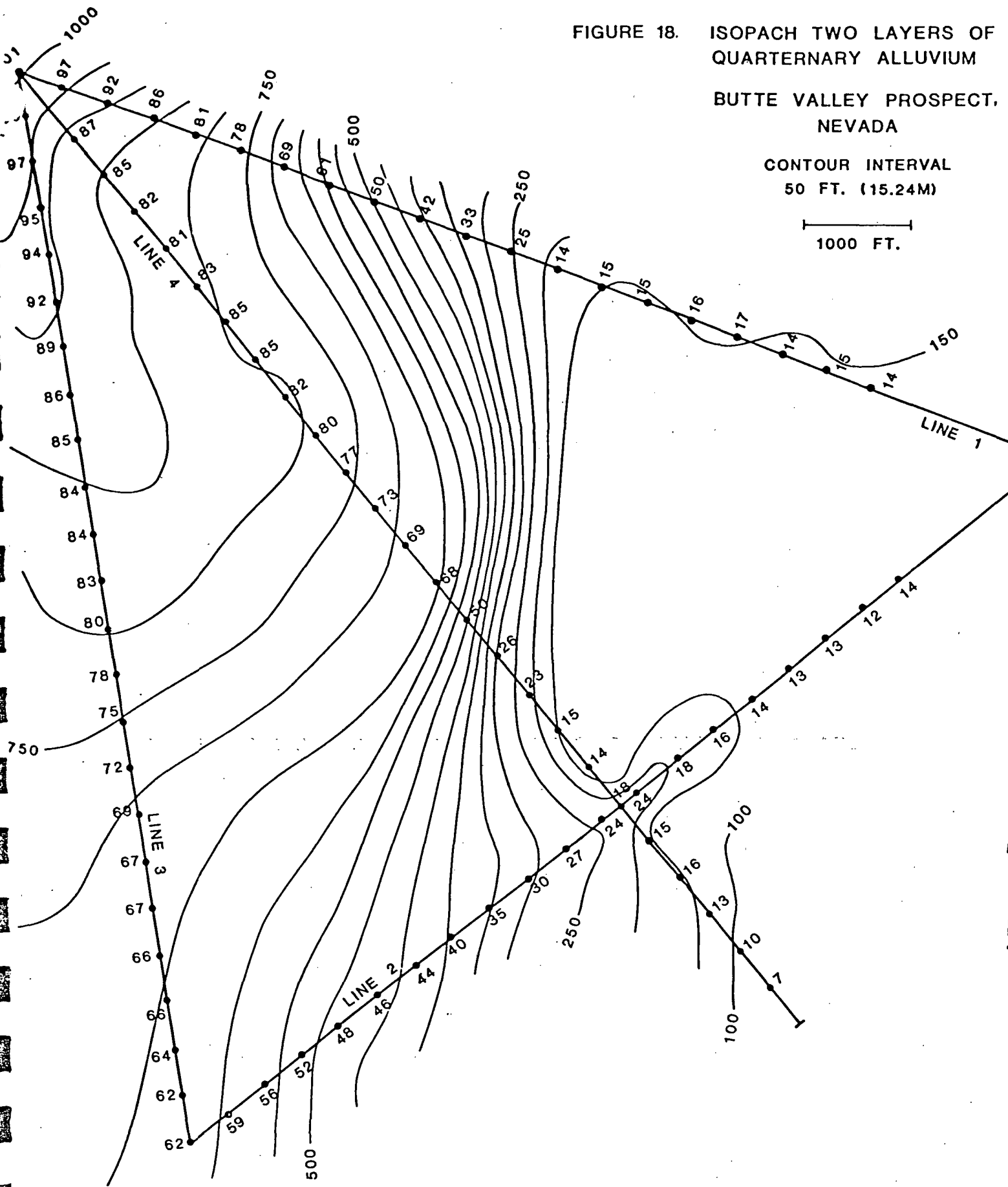
The isopach for the two layers of the Quarternary alluvium is plotted in Figure 18. The alluvium thickness varies from 30.5 m (100 ft.) in the south to 305 m (1,000 ft.) at the north apex of the triangle. The eastern portion of the survey area has an almost constant thickness of alluvium of 45.7 m (150 ft.). A significant fault crosses line 4 between stations 5 and 7 and line 1 between stations 8 and 11. In the line 2 solution, the fault is not as prominent. This fault at the base of the alluvium is the topographic feature seen in figure 4 with a 7 m relief.

The isopach for the combined Ely Limestone and Chainman Shale is plotted in Figure 19. These two lithologic units are combined because of their similar velocities (see Table 3). A greater confidence is placed in the isopach for the combined layers than in the separated isopachs. These lithologic units are also thinner to the east and southeast of the surveyed area. Thicknesses range from 12 m (40 ft.) to over 1070 m (3500 ft.) at the north apex of the triangle. A filled grabben with an additional thickness of 76 m (250 ft.) exists along line 4 near line 2. A thinning horst type structure occurs further to the north along line 4.

FIGURE 18. ISOPACH TWO LAYERS OF
 QUARTERNARY ALLUVIUM
 BUTTE VALLEY PROSPECT,
 NEVADA

CONTOUR INTERVAL
 50 FT. (15.24M)

1000 FT.



The northern side of this horst is a major fault extending from line 4 to line 1. The isopach thickens 150 m (500 ft.) to 300 m (1000 ft.) along the fault. Another major fault appears to exist parallel to line 1 with isopach thicknesses increasing 600 m (2000 ft.) to the north. From the refraction data alone, this northern fault must be interpreted with caution because it is based on data at the end of the line 4 refraction line. Near the ends of the profiles, there is less control than in the middle of the section. However, Welsh (1976) identifies this fault as the Caboose fault that dips 60 to 70 degrees to the northwest and is a normal fault with the northern side down dropped. The refraction data are in agreement with this geologically determined fault.

The isopach of the Diamond Peak Quartzite member of the Chainman Formation is plotted in Figure 20. This isopach is based mainly on data from line 4 with a confirmation of the trend from line 2 data. Thicknesses are about 30 m (100 ft.) on both ends and increase to 305 m (1000 ft.) in the center of the triangle. The isopach suggests a horst structure with thickening of the Diamond Peak Quartzite and thinning of the overlying Ely and Chainman (Figure 19). The profile along line 4 (Figure 14) indicates a thrust block of the Diamond Peak Quartzite. Because of the steep dips, gravity slide blocks, and thrust faulting in the area, either interpretation could be accepted from the refraction data.

The elevation of the top of layer 6 is contoured in Figure 21. This layer has an average velocity of 6294 m/s (20650 ft/s) and based on the drill hole data could have a lithology of quartz monzonite, Ely jasperoid, or Ely skarn. The elevations give a west northwesterly dip of about 12 degrees. With data from only lines 2 and 4, details are not available, but a complexity occurs near the intersection of the two lines with the contours pointing toward the area of high velocities determined from the fan refraction data (Figure 17).

FIGURE 20. ISOPACH DIAMOND PEAK QUARTZITE,
BUTTE VALLEY PROSPECT, NEVADA.

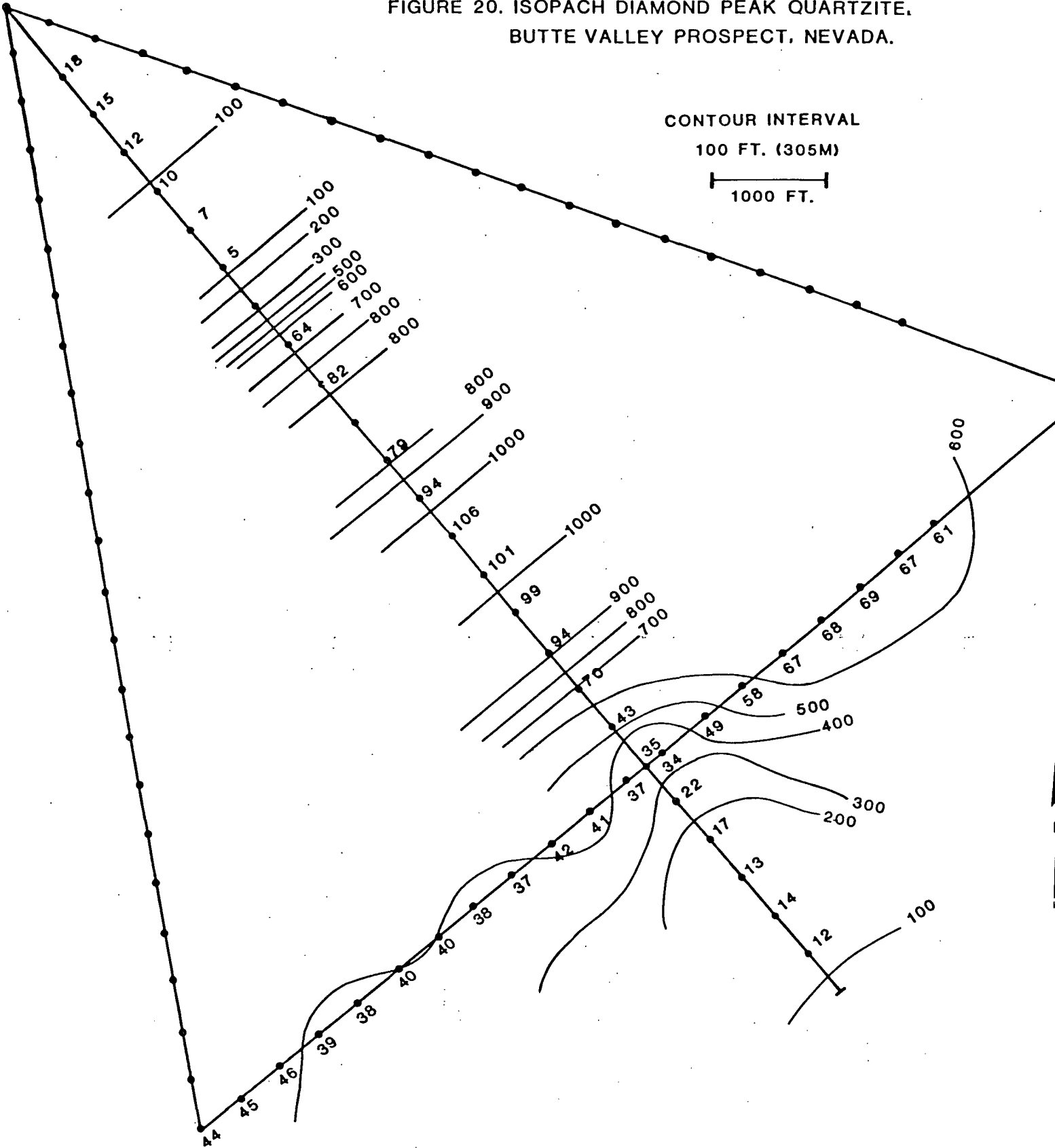
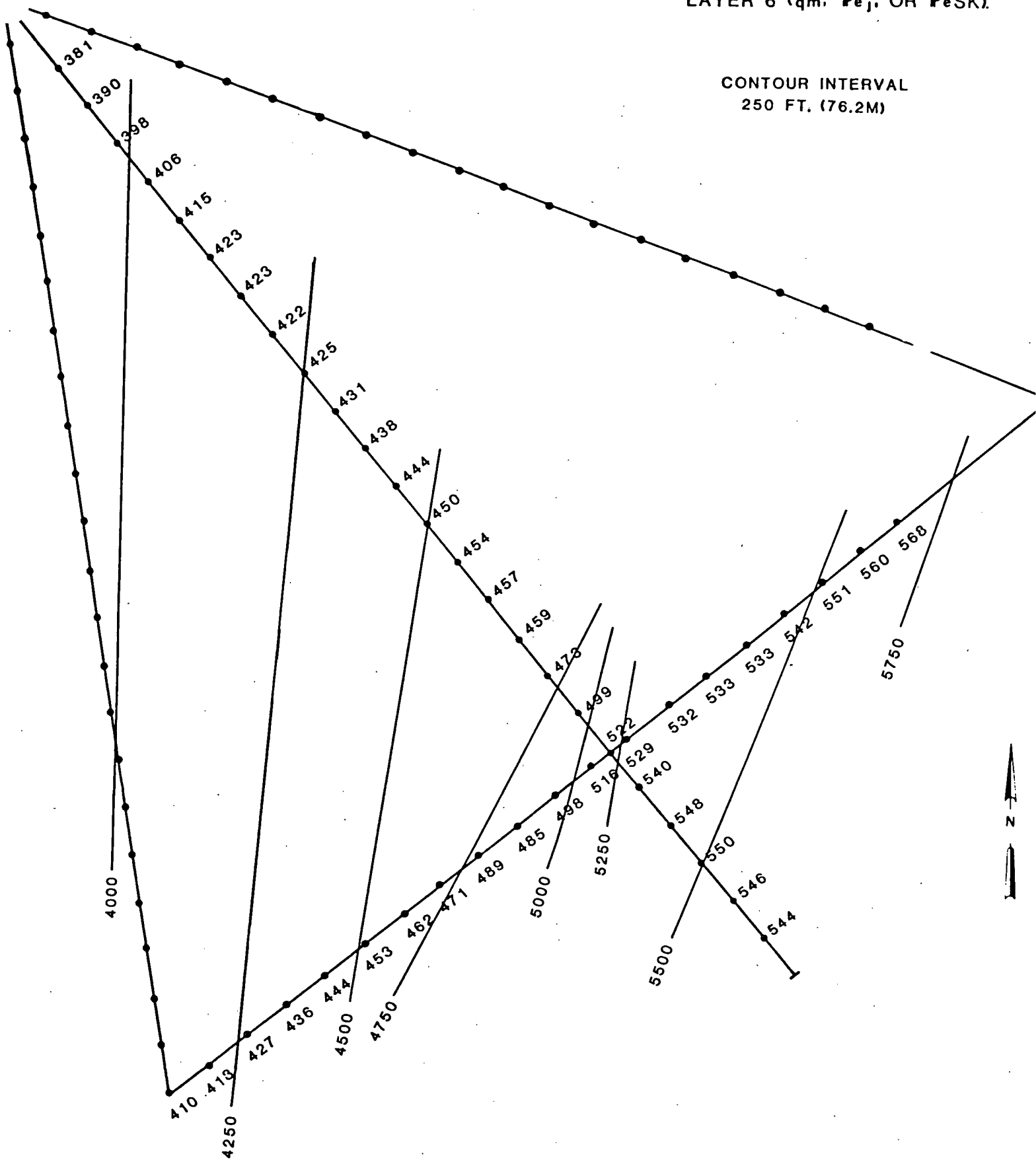


FIGURE 21. ELEVATION OF TOP OF 6294 M/S
LAYER 6 (qm, Pej, OR PeSK).



The thinning of both the alluvium (Figure 18) and the Ely-Chainman (Figure 19) to the east confirms the shallowness of the higher velocities to the east and southeast as seen from the fan refraction ray paths in Figure 17. The region in Figure 17 where the ray path segments from four shots overlap has the best possibility of being the center of the igneous intrusion. The region enclosed by a circular area enclosing the overlap of rays from three shots also has a high probability of being igneous or high grade metamorphic rock.

In summary, the general geologic interpretation from the refraction data is the identification of six layers with a complicated geological structure. Several major faults are identified that could be thrust faults or normal faults. Offsets on these faults of 75 m to 300 m are indicated. Velocities of 6300 m/s representative of competent igneous rocks are associated with the deepest penetrations. The structure dips steeply to the west with the depth of the 6300 m/s layer varying from about 150 m (500 ft.) in the east to about 670 m (2200 ft.) in the west. The most probable location for the stock is in the area of overlap of high velocity fan refraction rays about 610 m (2000 ft.) east by southeast of BV9.

V. REFLECTION STUDY

The reflection study is an independent seismic study. The reflection seismic method provides the best resolution of the subsurface geologic structure. Hence, it is the most important of the seismic methods investigated. The objectives of the study are given in Section A. The data parameters are listed in Section B. Section C contains the results in the form of three seismic cross-sections. The sections are interpreted in Section D, and the interpretation is summarized in Section E.

A. Objective

The primary objectives of the reflection seismic study are: to demonstrate the usefulness of this method in delineating the geologic structure; to suggest how a clear picture of the structure can help optimize drill hole locations for maximum ore sampling exploration; to evaluate resolution capabilities of the present advanced procedures of the oil exploration industry as applied to mineral exploration; and to consider methods and techniques of improving performance and of reducing costs.

A secondary objective of this study is to obtain preliminary data that can be used to investigate methods for interpretation of mineralized zones from the seismic response.

In meeting these objectives, it was considered essential to get the best quality records possible by proven methods. Consequently, experimentation to optimize record quality against survey costs was subordinated merely to obtaining the best efficiency with conventional practices.

B. Data

The data parameters are listed in Section III.

With the station spacing 34.3 m (112.5 ft.), the CDP point (reflection point) spacing is 17.1 m (56.25 ft.). Thus, the horizontal resolution is 17 m. The nominal fold of the data is six. Extra shots were fired at the ends of lines 4 and 5 to extend the full fold farther toward the ends of the lines.

The frequency content of the data was between the low cut filter of 16 Hz and about 75 Hz for most CDP points. At the ends of lines 4 and 5 where the alluvium thinned and the Ely Limestone outcrops, energy at frequencies up to 125 Hz is observed. The frequency content of the data was richer in higher frequencies with 0.23 kg (1/2 lb.) primer charges than with 2.3 kg (5 lb.) charges. The recording and amplifying systems were operated so that frequencies

The lithology is interpreted at the drill holes and in the immediate vicinity of the drill holes to illustrate the resolution of the structural details. These interpretations are made from the depths logged by Kennecott and from velocities determined from the refraction data. Apparently, the region has been subjected to a high temperature metamorphism. With this high degree of alteration, beds contain similar minerals and have lost the distinctive elastic contrasts that produce the clear reflections in the unaltered state. Because of the faulted structure and the small reflections in the relict beds, it is difficult to classify the reflection horizons far from the known lithology at the drill holes. The existence of relict beds and of faults is clear, but the lithologic identification is subjective.

The interpretation of the line 3 seismic section is given in Figure 25. The lithology of BV8, BV11, and BV13 is illustrated also in Figure 13 with the refraction inversion model. All three of these drill holes are close to line 3 but are not directly on the line. Note that north is on the right in Figure 25 and on the left in Figure 13. In the plane of the cross-section, the faults to the north dip to the south and the faults to the south dip to the north. The dips of these faults correspond to conjugate shear pairs. Several small pairs can be seen: one near the bottom of the BV13 projection, an inclined pair along BV11 and another set between BV11 and BV13. The key horizons in hole BV13 as logged by Welsh (1976) are the 76 m (250 ft.) thick olivine basalt at a depth of 500 m (1640 ft.) and the 9 m (30 ft.) thick basalt at a depth of 685 m (2280 ft.). The seismic section suggests that the lower basalt could be the top of a cut off, faulted section downthrown 185 m (640 ft.) to the north and not a second thinner basalt layer. The Ely Limestone interpreted at 0.22 s appears in Welsh's lithologic log of BV13 as "fanglomerate: limestone, chert, sandstone cobbles." Miller's (1971) illustrations for BV-13 include the Ely. BV-13 is about 160 m (520 ft.) east of line 3 and will not provide complete detail on this line. The projection

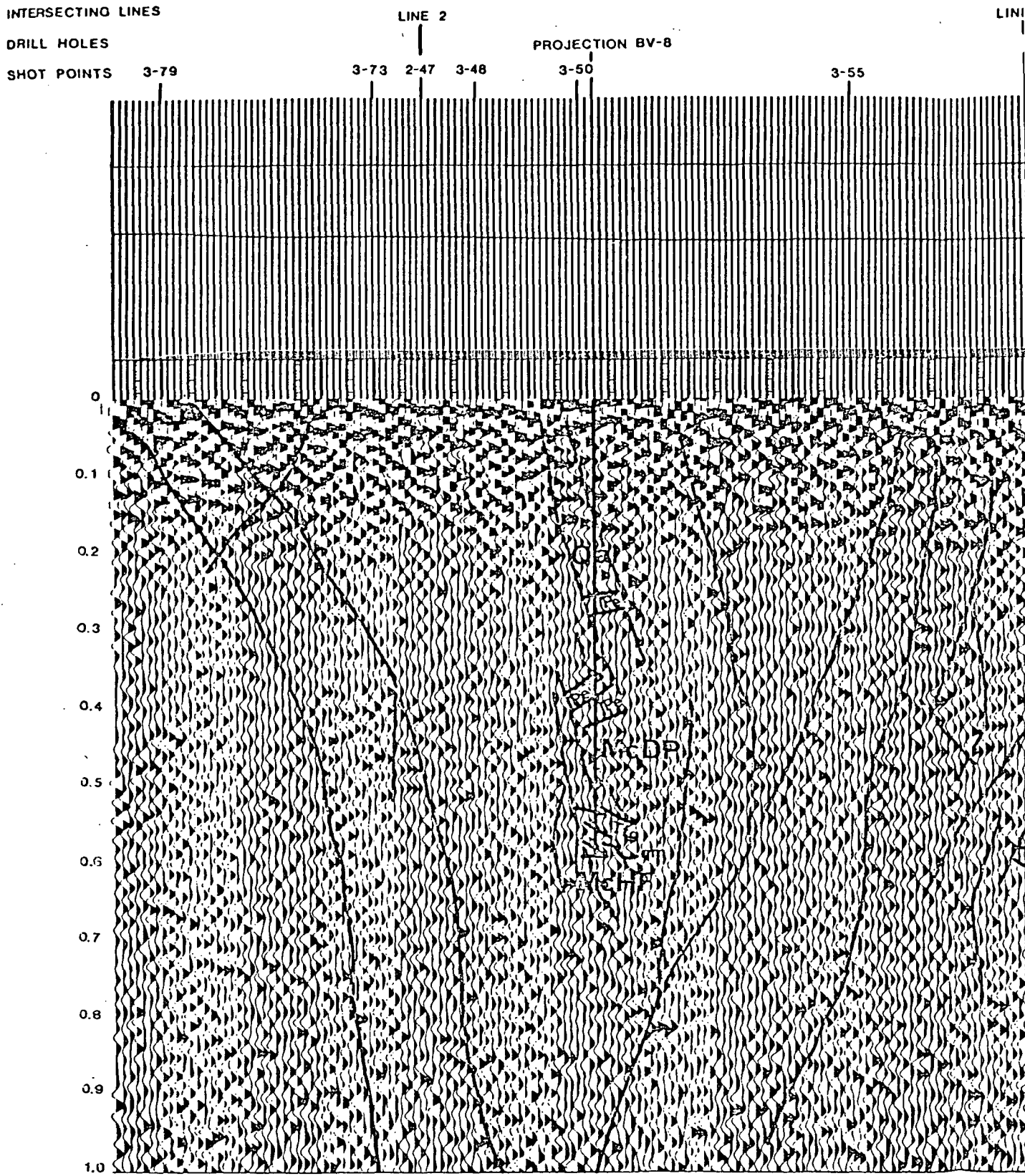


FIGURE 25. LINE 3, BUTTE VALLEY, NEVA

INTERSECTING LINES

DRILL HOLES

SHOT POINTS

LINE 2

PROJECTION BV-8

3-79

3-73

2-47

3-48

3-50

3-55

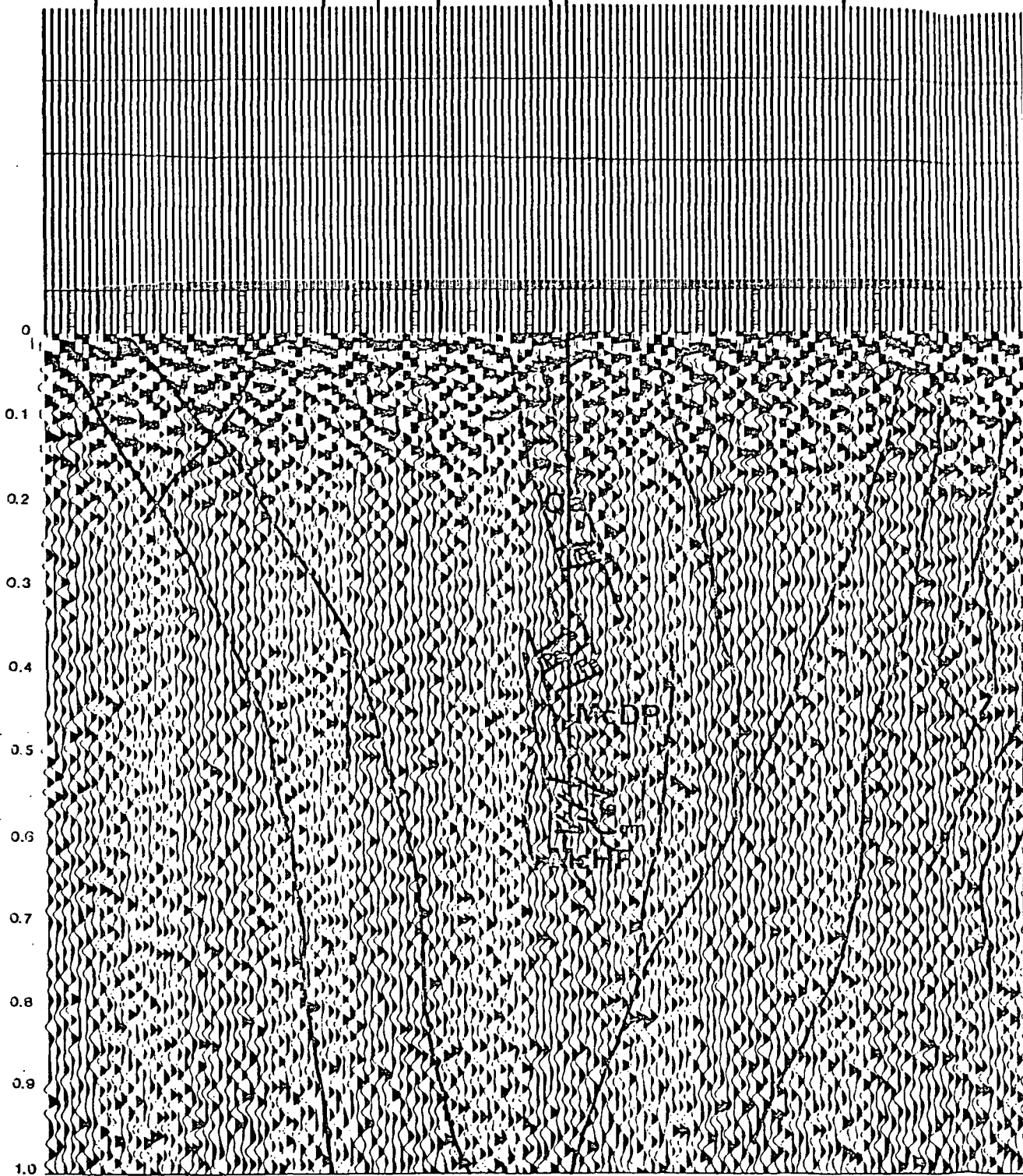


FIGURE 25. LINE 3, BUTTE VALLEY, NEV.

LINE 5
PROJECTION BV-11

LINE 1 & LINE 4
PROJECTION BV-13

3-60

3-85

3-69

1-1

3-91

3-93

ELEVATION (FT)
6400
6300
6200

FOLD

0

0.1

0.2

0.3

0.4

0.5

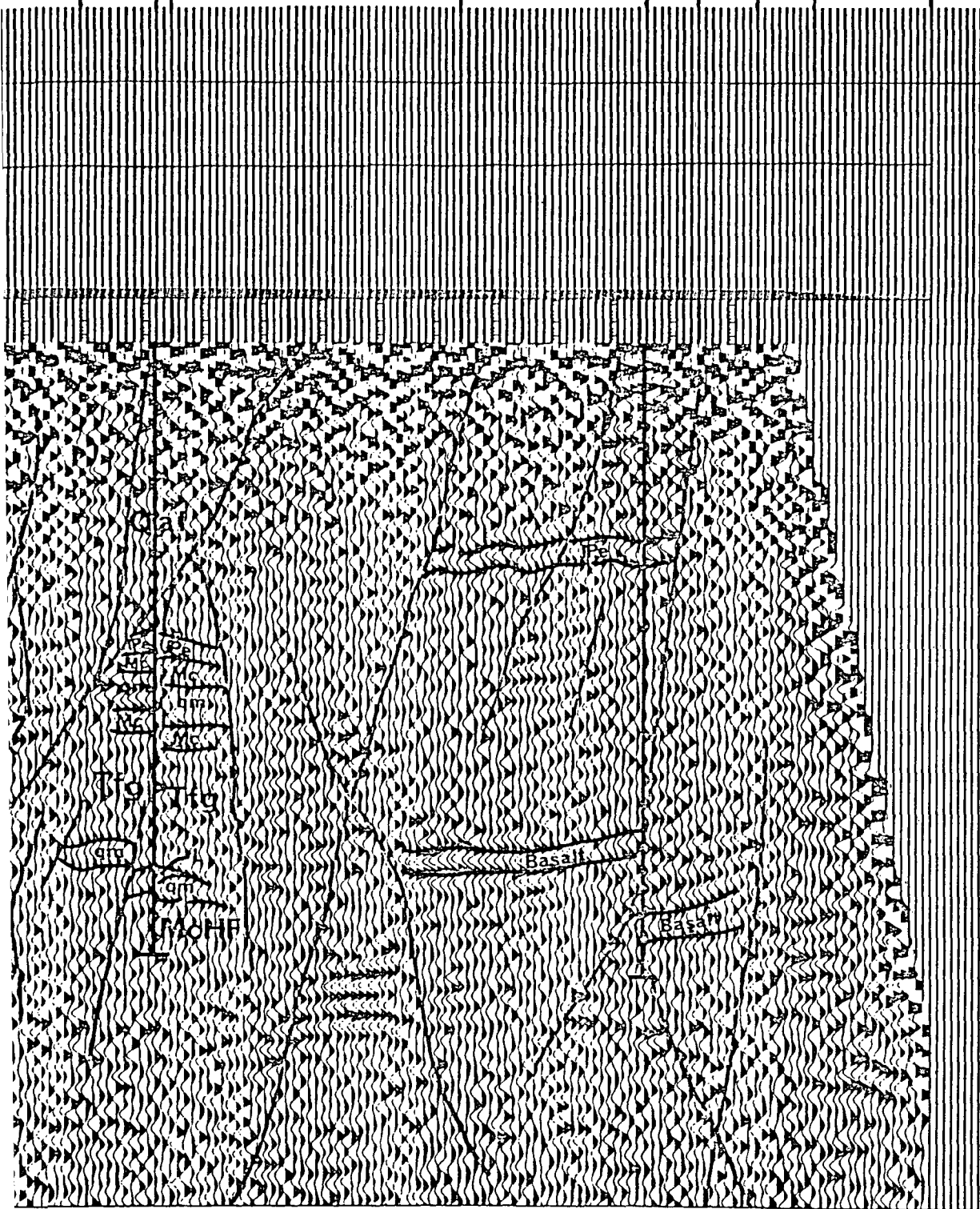
0.6

0.7

0.8

0.9

1.0



NEVADA, INTERPRETED SEISMIC SECTION

of BV11 also lies along a fault with the north side downthrown. The Tertiary fanglomerate (Tfg) section could appear thicker in the drill hole because of the relationship between the fault and the borehole. There is good correlation with the lithology on both sides of the fault, but extension of the interpretation beyond the nearby faults becomes speculative. The 16 m (48 ft.) thick latite (L) appears to be delineated only in the immediate vicinity of BV11. (This 16 m thick bed is the smallest vertical dimension identified in the three sections.) The strong set of 5 reflection horizons between 0.7 and 0.8s south of station 3-65 are cut off by a conjugate shear set of faults. These reflections are different from others on all three sections and are unidentified. At BV8, the lithology of the alluvium and the top of the Ely Limestone is questioned by Welsh (1975). The seismic section has been interpreted as a vertical sequence of en echelon faults that repeat the Ely Limestone section. The thickness of each individual section is about 25 ms as correlated at the other drill holes. The repeated sequence could explain Welsh's logging of 143 m (470 ft.) of Ely Limestone in BV8 as compared to 48 m (156 ft.) at BV11 and 43 m (140 ft.) at BV9. The connection of the quartz monzonite (qm) sill and the underlying Chainman Hornfels between BV8 and BV11 is not at all clear in the seismic section. The top of the Tertiary fanglomerate has been interpreted by Welsh (1967) and Miller (1971) as the contact of the gravity slide block. The continuity of this surface has been distorted by significant faulting since the slide took place. Also, the indistinctness of this sharp discontinuity in the reflections suggests the possibility of additional widespread metamorphism following the regional westward tilting and subsequent gravity sliding. These events have not been previously recognized. (See Miller's 1971 chronology of events summarized in Section II.A.). The fault at the southern end of line 3 is the fault related to the topographic relief seen in the aerial photograph in Figure 4.

The interpretation of the line 4 reflection seismic section is given in Figure 26. The lithology of BV13, BV10, BV9, BV14, BV2 and BV5 is illustrated also with the refraction inversion model in Figure 14. This section contains many faults with high angles and with vertical conjugate shear patterns. Vertical en echelon faults are interpreted at BV1, BV5, and BV2 to create the apparent greater thickness of the Ely Limestone as contained in the well logs. The Chainman Shale formation is also cut by parallel faults. Both the Diamond Peak Quartzite member and the Chainman Shale member occurred in BV2. Whereas, only the Diamond Peak appeared in BV5 and only the Chainman Shale appeared in BV1. The many faults in this area aid in interpretation of these changes among nearby drill holes. The Tertiary fanglomerate is a thin bed at these three drill holes. It is underlain by an Ely Skarn in BV2 and BV5. The BV2 drill hole bottomed in the skarn. Welsh (1972) reports dips of 30 to 45 degrees in the upper 76 m (250 ft.) of the Ely Skarn in BV5 with dips averaging 70 degrees. The Ely Skarn also contained frequent shear zones that were probably related to the steep dips. Welsh (1972) reports uniform dips of 40 to 45 degrees in the Ely Skarn in BV2. Steep dips are evident from the seismic data. The BV5 drill hole intersected altered beds from the early Mississippian and the late Devonian in the Chainman Hornfells, the Joana Limestone altered to Joana Jasperoid and the Devonian Pilot Shale altered to Pilot Skarn. These beds are in the apex of intersecting faults and apparently have been faulted up into the more recent section. The drill hole BV1 did not intersect the Ely Skarn but passed through the Chainman Hornfells and bottomed in the quartz monzonite. Drill hole BV14 is on the edge of the topographic relief seen in the aerial photograph in Figure 4. The fault related to this feature is almost vertical in the plane of the section. The lithology is nominal in BV14 for the alluvium, the Ely Limestone, the Diamond Peak Quartzite, and the Chainman Shale. The Tertiary

INTERSECTING LINES

DRILL HOLES

SHOT POINTS

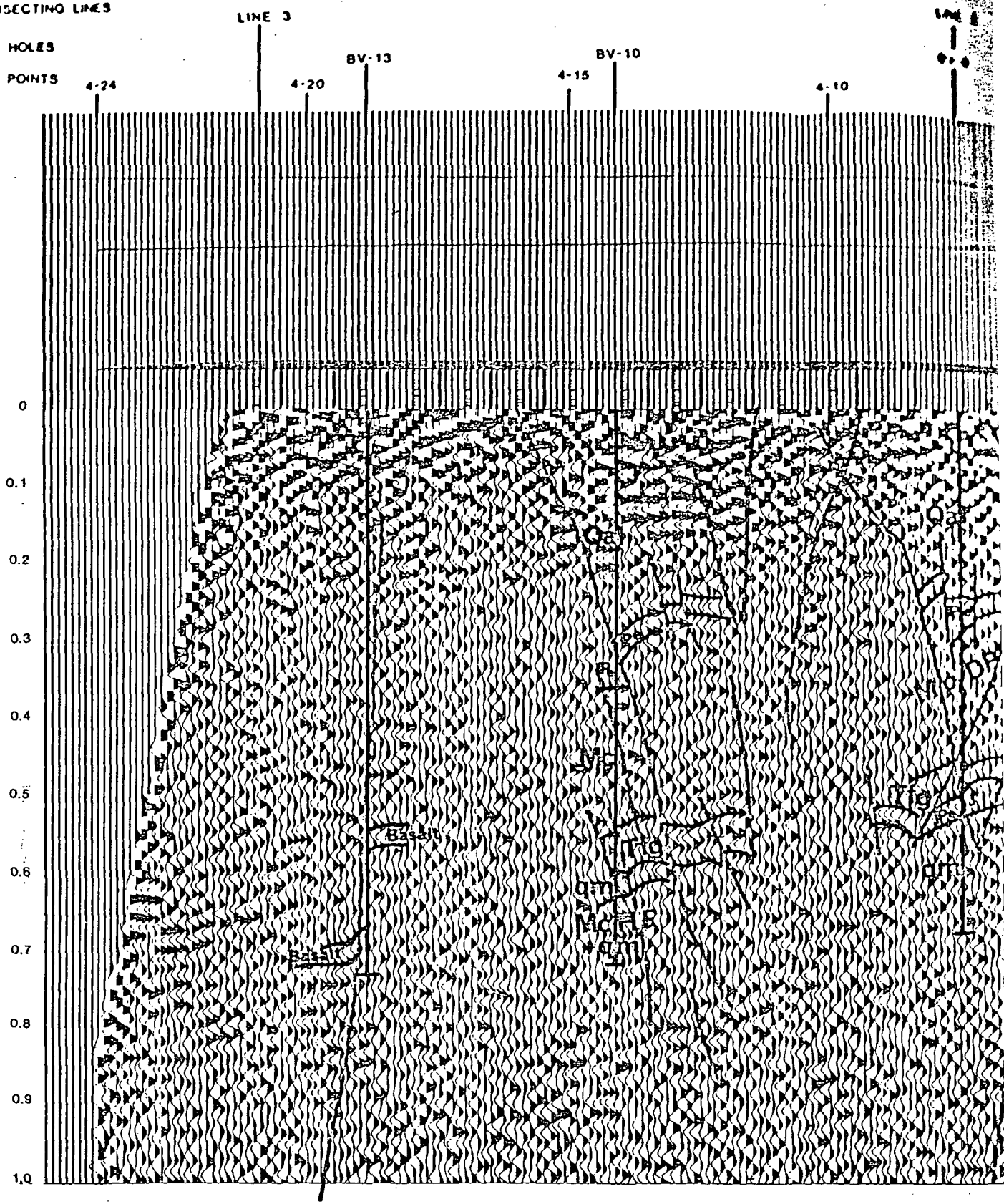
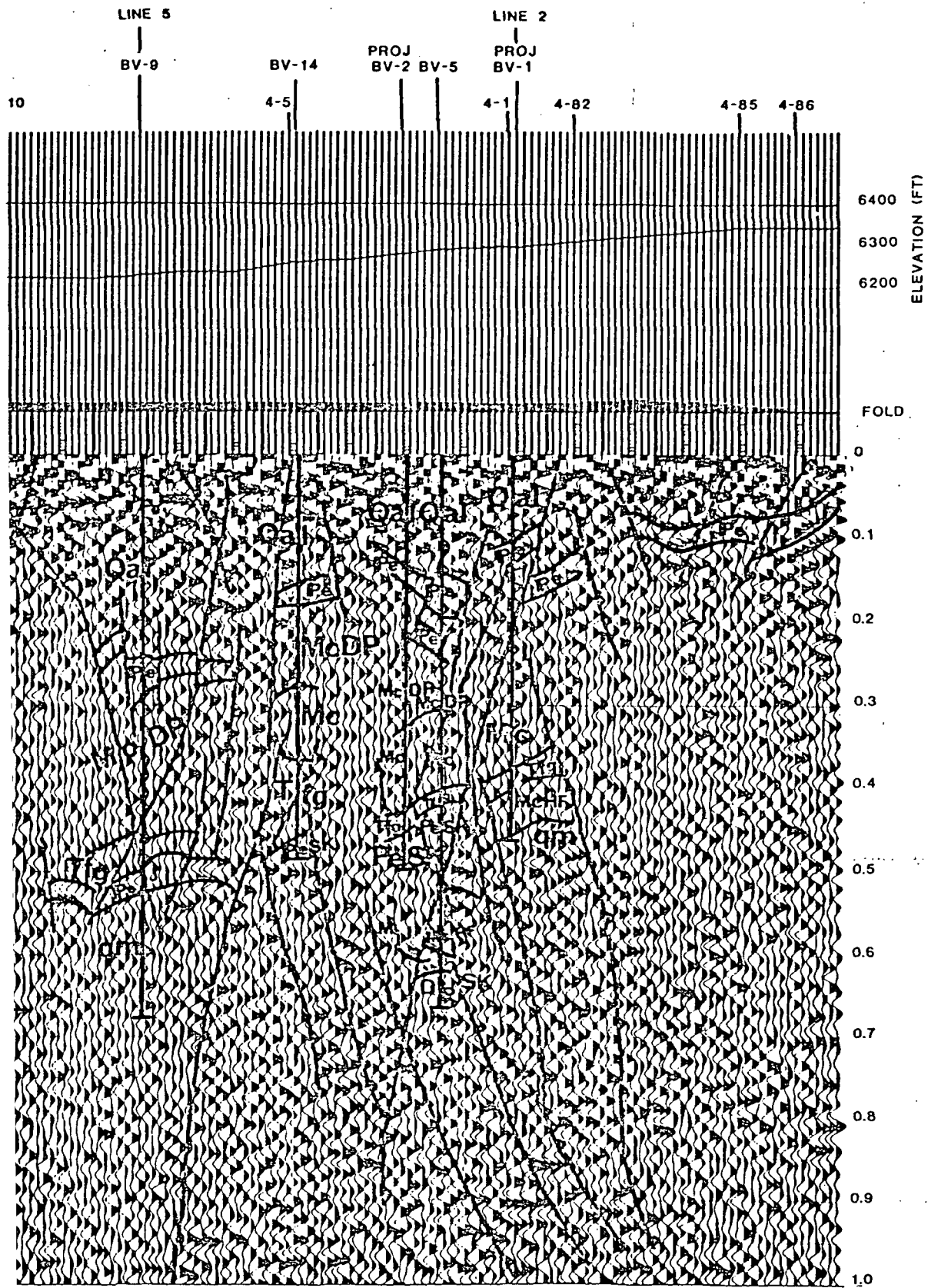


FIGURE 26. LINE 4, BUTTE VALLEY, NEVADA, IN



1/ADA, INTERPRETED SEISMIC SECTION

fanglomerate has a thicker section than elsewhere and could have some repetition of section with the fault that crosses the hole within the fanglomerate. BV14 terminates in the Ely Skarn. The major fault with the surface expression is between drill holes BV9 and BV14. The Ely Limestone, Diamond Peak Quartzite, and Tertiary fanglomerate are all upthrown at BV14 relative to BV9. BV9 intersects the Ely Skarn and bottoms 392 m (1287 ft.) into the quartz monzonite. Drill hole BV10 is cut by faults with a dominant dip to the southeast in the plane of the section. The apparent thicker section of Ely Limestone is again interpreted as a repeat section resulting from closely spaced parallel faults. The Diamond Peak Quartzite is absent but the Chainman Shale is present. The Tertiary fanglomerate may also be thickened by fault repetition of the section. The quartz monzonite is 113 m (372 ft.) thick. BV10 bottoms in the Chainman Hornfels that contain quartz monzonite inclusions. The lithology of drill hole BV13 is logged as a sequence of fanglomerates by Welsh (1976). This hole penetrates a fault for much of its depth. A possible explanation for the deviation from the normal lithology is that the samples from BV13 are predominantly a fault gouge that contain cobbles and other flour ground from the country rock. The line 4 section interpretation of the two basalt sills is that they are probably one sill offset 185 m (640 ft.) by the fault. This interpretation is in agreement with the line 3 section interpretation in Figure 25. The general structure of line 4 pictured in Figure 26 is beds dipping down to the northwest; complex faulting that occurs on high angle faults with two sets of dips in conjugate shear relationships; some repeated sections from parallel faults that generally are upthrown to the southeast but with a few downthrown segments; and an anomalous segment of late Mississippian and early Devonian beds displaced upward in the section.

The interpretation of the line 5 reflection seismic section is given in Figure 27. The most significant difference between line 5 and lines 3 and 4 is the clear reflections on the western end of the line. Line 5 starts well out in the valley at the intersection of the two 1955 Gulf lines. The upper set of reflections are interpreted as the Pennsylvanian Ely Limestone and the Mississippian Chainman Formation. The lower set of strong reflections between 1.1 and 1.4 s (see Figure 24) are the Devonian Guilmette Formation that contains numerous limestone and dolomite sequences. A most interesting feature is that the parallel beds separate with the upper beds dipping upwards and the lower beds dipping downward. Almost all of the beds cease to be good reflectors from the vicinity of station 5-29 to the southeast. The combined deformed structure and change in elastic parameters suggest that the intrusion of the igneous rocks has caused a sufficiently high grade of metamorphism to alter the host rock mineral assemblages well into the valley. Inspection of Figure 4 reveals that station 5-29 is well removed from the vicinity of the exploration drill holes. Similar to lines 3 and 4, line 5 has numerous faults that have two sets of dips with conjugate shear relationships. The geometry of the faults is consistent with a major stress in the vertical direction. However, the separation of the flat lying beds to the west also requires a significant horizontal force. The most recently completed drill hole, BV15, is cut by faults in the upper section. The lithology logged by Welsh does not list the Ely Limestone. According to the seismic interpretation, the Ely terminates at a fault in the vicinity of the drill hole. The Diamond Peak Quartzite is only 27 m (90 ft.) thick. The Chainman shale is present and is underlain by a latite with an oxidized limonite capping. BV15 bottoms in the Chainman Hornfels. A set of conjugate shear faults is between BV15 and BV9 at about 0.6s. The quartz monzonite apparently is terminated by this fault

INTERSECTING LINES

DRILL HOLES

SHOT POINTS

LINE 3

BY

5-35

5-30

5-25

5-20

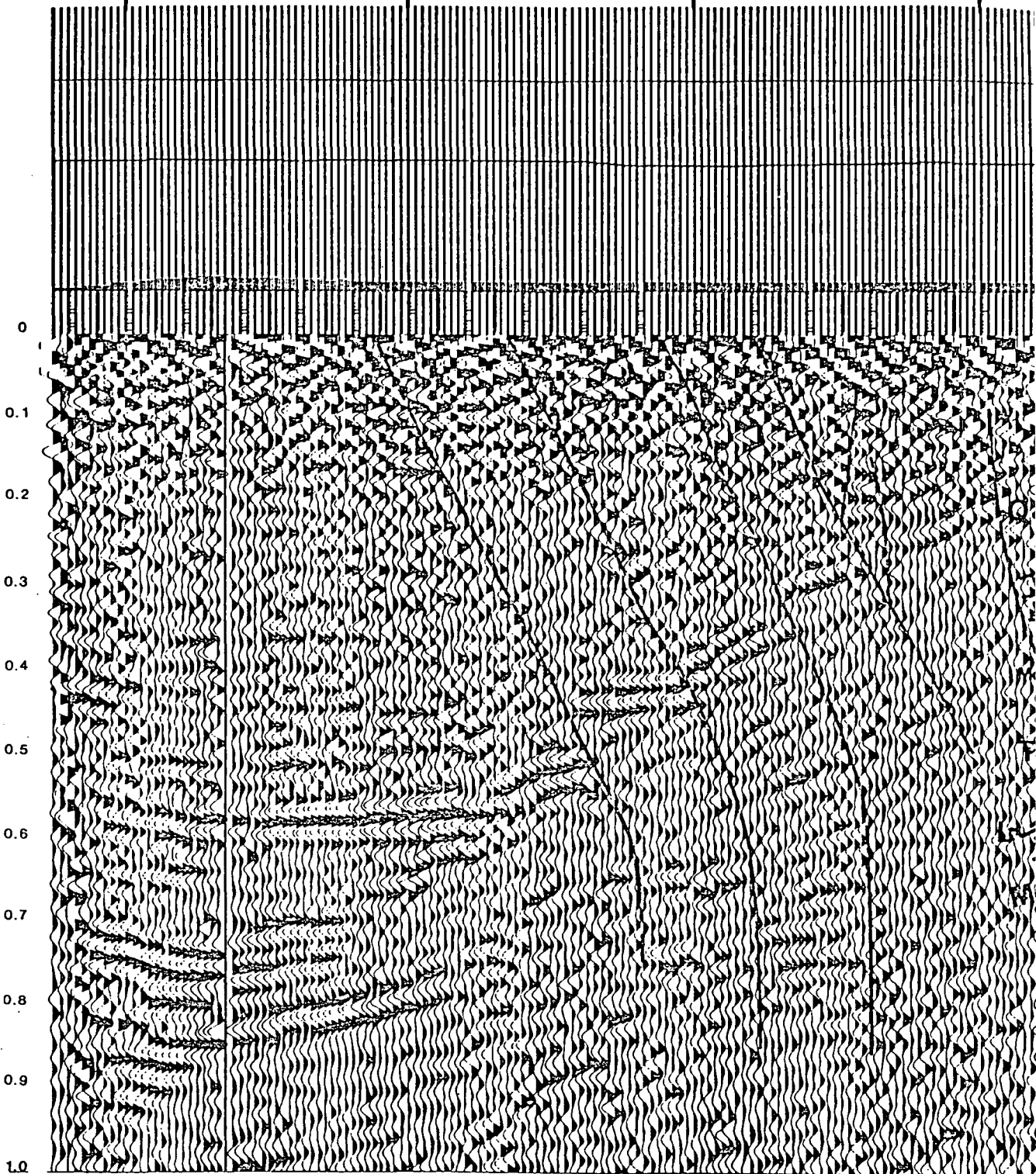
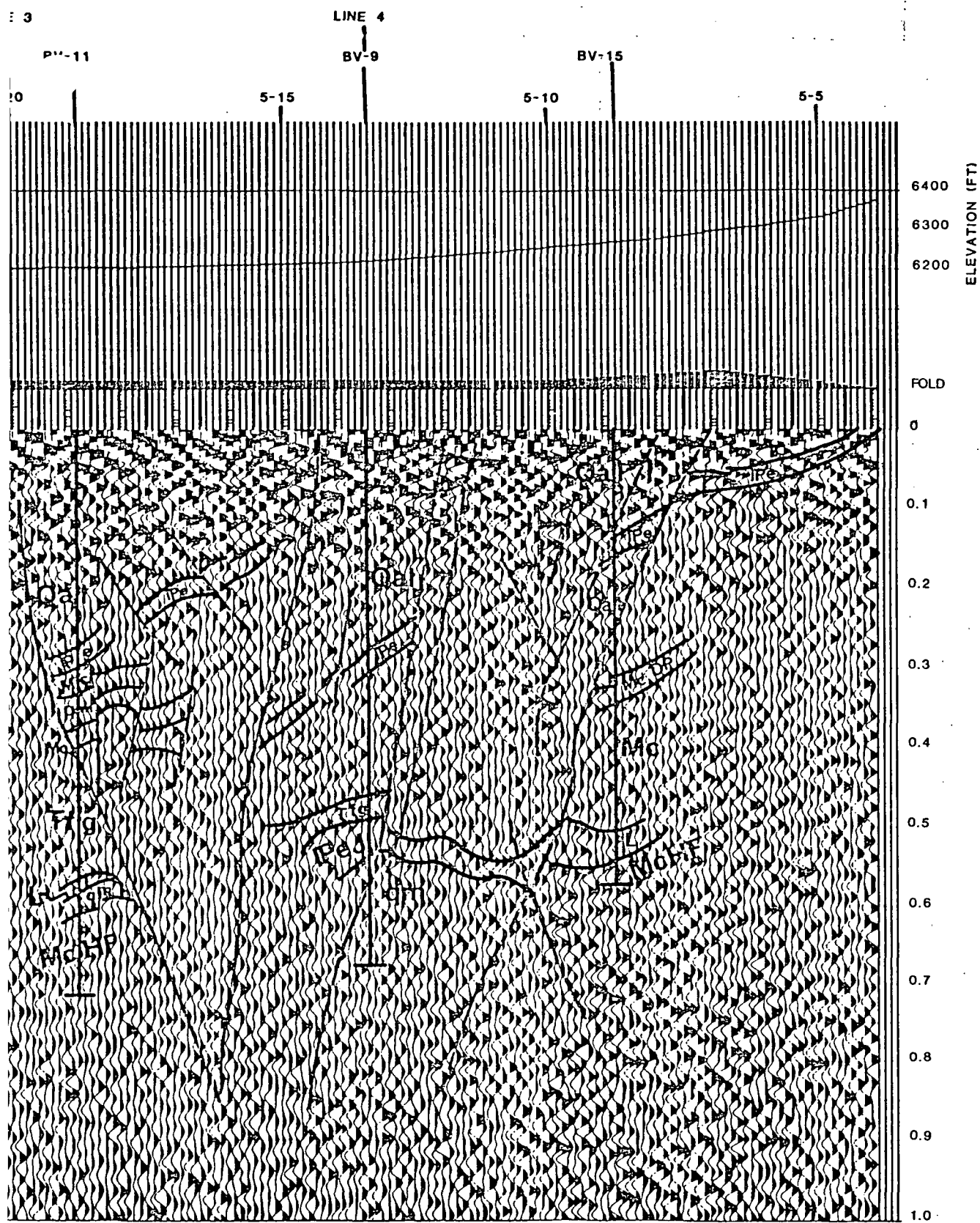


FIGURE 27. LINE 5, BUTTE VALLEY, NEVADA



NEVADA, INTERPRETED SEISMIC SECTION

to the east. The fault with the surface topographic relief is to the east of BV9 at the surface and intersects the drill hole in the quartz monzonite. The lithology of drill holes BV9 and BV11 were discussed above. The interpretation in the line 5 section is in agreement with the previous interpretations.

With the aid of the seismic reflection sections the surface trace of three faults can be identified in the aerial photograph of Figure 4. The fault with the 7 m topographic relief has been referred to before. This fault trace cuts line 3 at station 3-80, the southern end of the line, line 4 at station 4-5, and line 5 at station 5-12. This fault is clearly defined on the three interpreted sections in Figures 25, 26, and 27. Another fault trace is about 650 m (2000 ft.) west of the above fault trace and strikes about N20E. This trace appears as a fault zone in Figure 4. In a direction from south to north, the zone starts as a line of dark gray grass, continues across a lighter grass as a 200 m (650 ft.) wide line of sagebrush, crosses line 3 to the southeast of BV8 at about station 3-50, intersects BV8 in the subsurface as seen in Figure 26, continues at the edge of a color change in the sage brush, passes to the east of BV3, changes direction parallel to the first fault, intersects line 5 at station 5-15-2 to the west of BV9, disappears under the presently forming fanglomerate, but is seen in Figure 27 to intersect line 4 at station 4-9-2 in line with the fault on the aerial photograph. Both of the first two faults dip to the northwest. The third fault trace is parallel to the first two faults and is about 1750 m (5800 ft.) farther west. This fault dips to the southeast. The region between these three faults with surface traces could be significant to the continued exploration of the Butte Valley Prospect. The trace of the third fault starts in the south of Figure 4 as a line of sagebrush along the east side of an apparent drainage channel. This

line of sagebrush continues across line 5 near station 5-23, then crosses line 3 at station 3-62-2, the trace is seen as a single width of sagebrush across the grass intersecting line 4 at station 4-16, and disappears midway between lines 4 and 1. The continuation of the third fault across the recent fanglomerate to the north of line 4 suggests that tectonic activity is still continuing at the present. The continued movement on the faults should facilitate groundwater flow and continue to enhance secondary enrichment. The identification of these three fault traces is a significant contribution of the seismic survey.

E. Interpretation Summary

The details of the physical structure reveal a complicated faulted sub-surface with considerable folding. The faults are in conjugate shear relationships that result from a large upward vertical force probably created by the injection of the intrusive bodies. Separation of flat beds to the west also indicates significant horizontal forces secondary to the primary vertical force. A much more complicated structural relationship is interpreted from the seismic data than was possible from only the lithological data from the sixteen drill holes. In many locations, parallel faults occur in an en echelon manner; beds are repeated within the drill holes and have led to interpretations of thickening sections rather than repeated sections. The direction of relative motion on the closely spaced faults is not always the same. The general trend is for upthrown displacements to the east and southeast, but occasionally an intermediate segment will not have as much displacement as adjacent segments on either side. The faults cut all identified lithologic units including late Tertiary basalts and recent fanglomerates. This fact indicates additional tectonic activity after the gravity slide and requires an addition to the major geologic sequences described by Miller (1971) and summarized in Section II.A1.

Although the faults are reasonably defined, the high grade of metamorphism has altered the mineralogy so that at the present, the lithology can be identified only in the vicinity of the drill holes. There are distinctive characteristics to some of the reflections and possibly with future research into velocities and elastic properties of rocks occurring in porphyry copper systems methods of recognizing specific lithologic characteristics can be established.

Concentric alteration zones as described in the model of Lowell and Guilbert (1970) and illustrated in Figure 2 are not evident in the seismic sections. However, the Butte Valley structure is similar to the structure in the Robinson district as described by James (1976) and as generalized in Figure 3. In several locations, the quartz monzonite is terminated by a fault and is in contact with altered country rock. Many small faults occur near each other. There are suggestions both in the seismic sections and in the drill hole lithology that some of the faults may contain large amounts of gouge. The high angle faults are common to both regions. The ample abundance of active faults provides good possibility for secondary enrichment through ground water flow in faults kept open by repeated movement.

One serious consideration that warrants further investigation is that there are reflections with linear continuity immediately below the identified quartz monzonite. Are these reflections from layering or faulting within the intrusive body or are they relict sedimentary beds and the monzonite is limited in vertical extent? The longest penetration of the monzonite was 392 m (1287 ft.) at the bottom of BV9. The linear continuity of reflections in this interval is rather weak, but there are parallel reflections at about 0.725 and 0.755s immediately below BV9.

VI. MAGNETIC STUDY

This study of the total magnetic field at the Butte Valley Prospect is presented to illustrate the possibilities of improving the overall geophysical understanding and interpretation by combining the seismic results with other geophysical data. This study is only a preliminary, brief investigation to demonstrate the possibilities of an integrated approach. These magnetic and seismic data could provide a good data set for a more detailed investigation of the inter-relationship at a porphyry copper deposit.

The Butte Valley Prospect was originally located as a magnetic anomaly from data taken by Gulf at a high altitude in a regional study. Kennecott has taken additional aeromagnetic and surface data. The aeromagnetic data were used for this study. Because of the mountains, the data were taken at two flight elevations -- 2286 m (7500 ft.) and 2743 m (9000 ft.) -- and were plotted together. The Kennecott contour maps were hand digitized in a 305 m (1000 ft.) grid. The data at the higher elevation were filtered, downward continued, and refiltered. The mean was removed from both segments; they were joined and migrated to the pole. The resulting contour map is plotted in Figure 28*. The circular anomaly near the center is over the prospect. The location of lines 3, 4, and 5 is shown on the map. The match between the two portions is good at this anomaly but is not an exact match all along the joining line. Profiles approximately along the seismic lines were extracted from the contour map and are plotted at the top of the seismic sections in Figures 22 to 24.

The anomaly along line 3 has an amplitude similar to that along the other lines. The peak of the anomaly occurs between faults that have opposite dips in a conjugate shear relationship. A quartz monzonite sill was intersected in BV8 within the center third of the anomaly.

*Figure 28 is in the attached folder.

The anomaly along line 4 peaks in the vicinity of BV5 and BV1. The quartz monzonite was intersected in BV1 but not in BV5, BV2, or BV14. Altered minerals containing magnetite were encountered in all three holes.

The anomaly along line 5 has an artificial double peak caused by the joining of the two sections. The quartz monzonite was intersected in drill holes BV11 and BV9. These two drill holes are separated by two faults with opposite dips. BV15 did not intersect the monzonite but bottomed in altered Chainman Hornfels.

To model the line 5 anomaly, an approximate shape was taken from the reflection section as illustrated in Figure 29. Dimensions were approximated from the drill hole data and the seismic section. The total magnetic field reduced to the pole at an elevation of 2286 m (7500 ft.) was calculated for the model and is illustrated in Figure 30 with the observed anomaly plotted to the same scale. In the first calculation for the model, a susceptibility of $16,000 \times 10^{-6}$ cgs as determined by Wright (Frangos and Wright, 1972) was used. However, to obtain the fit in Figure 30, the susceptibility for a uniform body had to be reduced to $2,320 \times 10^{-6}$ cgs. In the model, this represents a susceptibility contrast between the modelled shape and the surrounding rock.

As stated above, this study of the magnetic field is only a brief investigation to illustrate the possibilities of joint interpretations with seismic and magnetic data. No attempt has been made here to establish two dimensional models for lines 3 and 4 or a three dimensional model for the entire anomaly or to investigate the order of magnitude differences in model apparent susceptibilities. An extension of this brief study would be beneficial for continued geophysical evaluation of the prospect.

INTERSECTING LINES

DRILL HOLES

SHOT POINTS

5-35

5-30

5-25

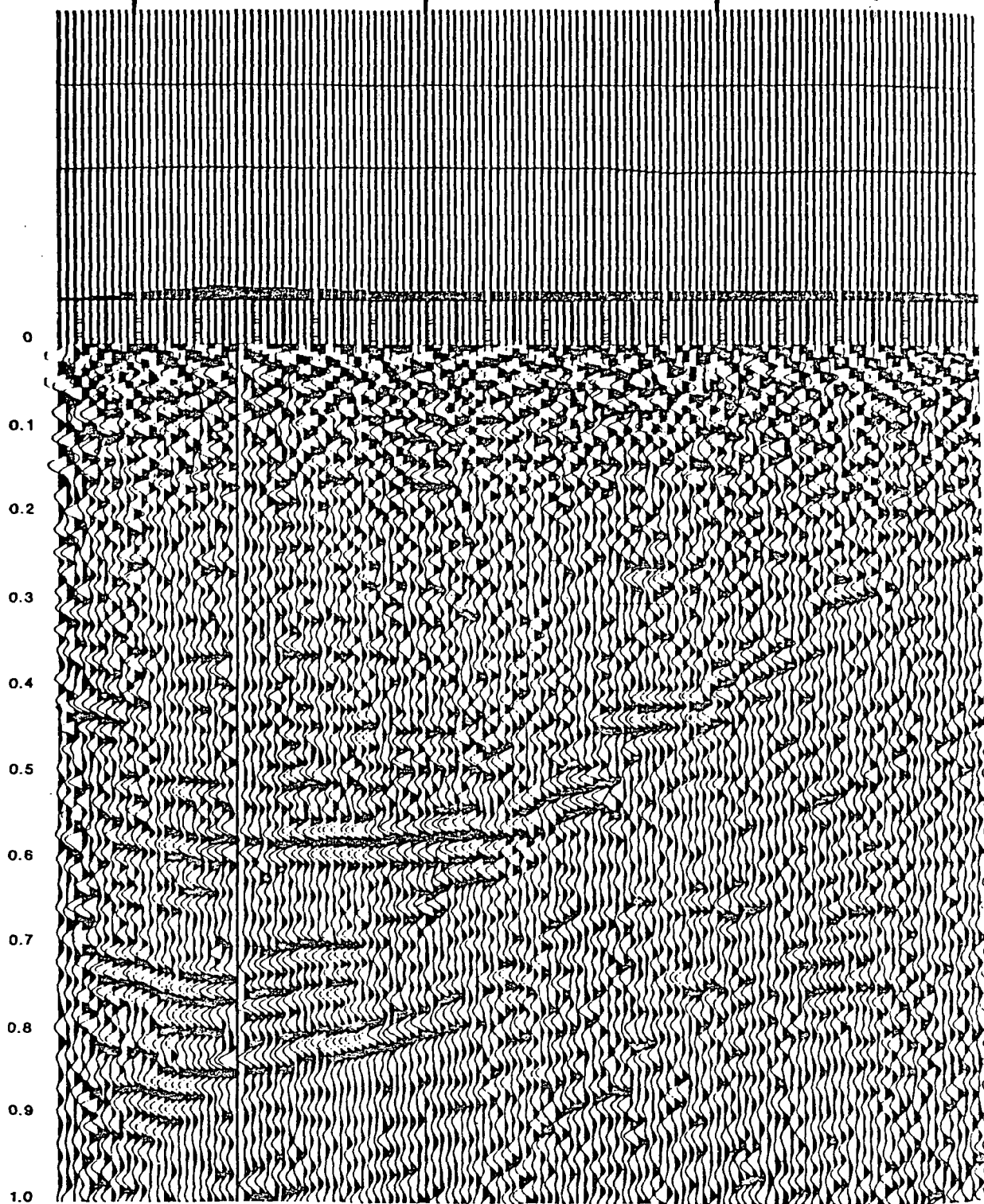
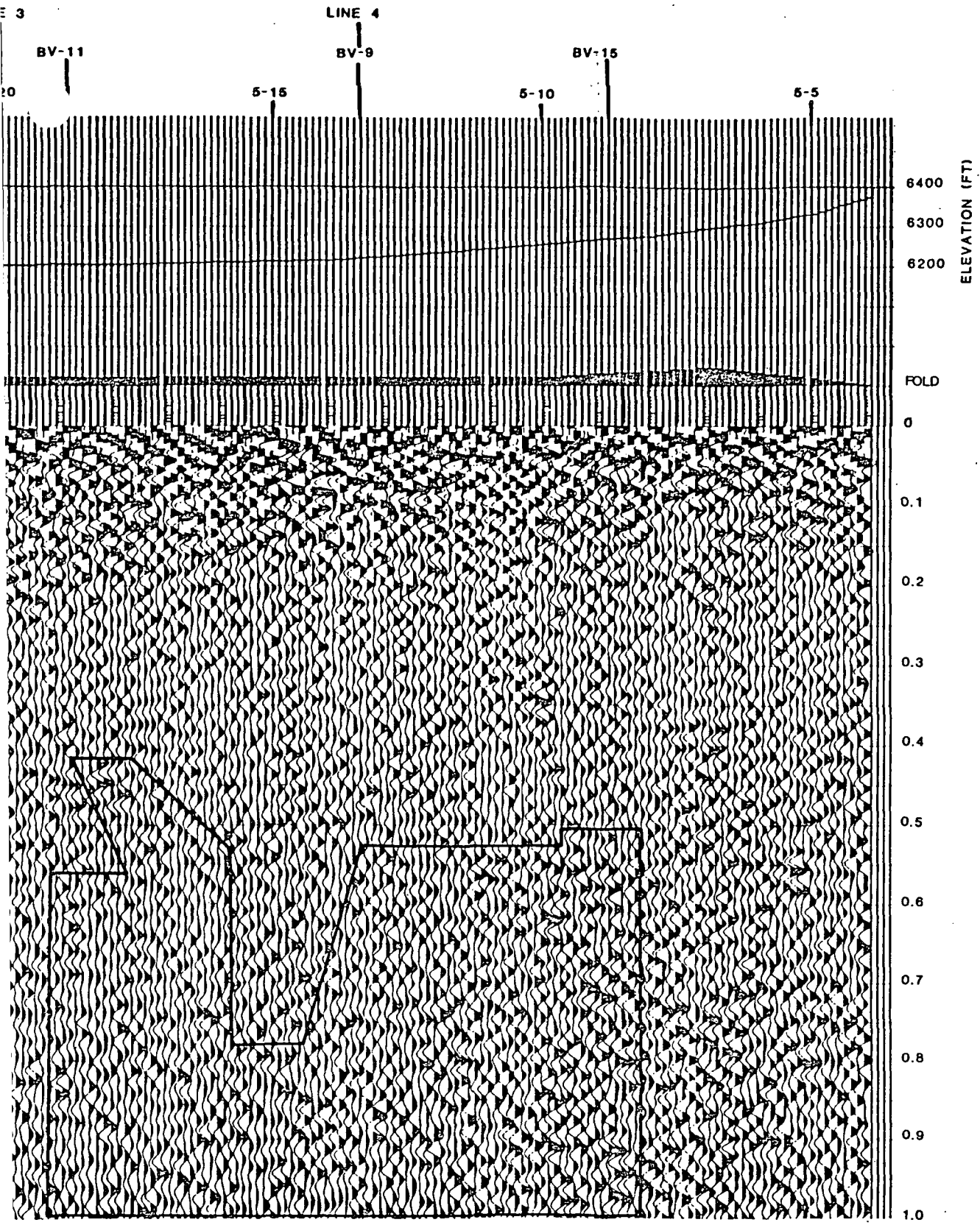


FIGURE 29. APPROXIMATE SHAPE ON SEISMIC SECTION,



F MAGNETIC MODEL SUPERIMPOSED
IN 5

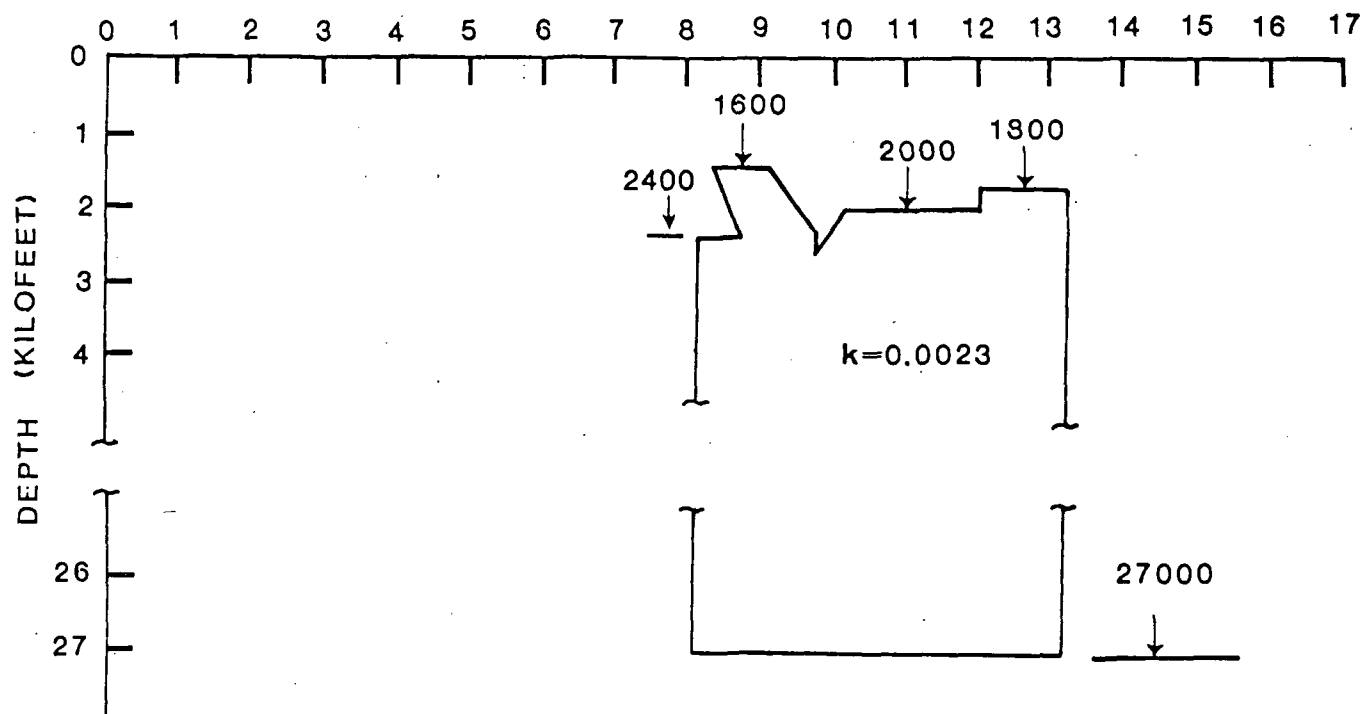
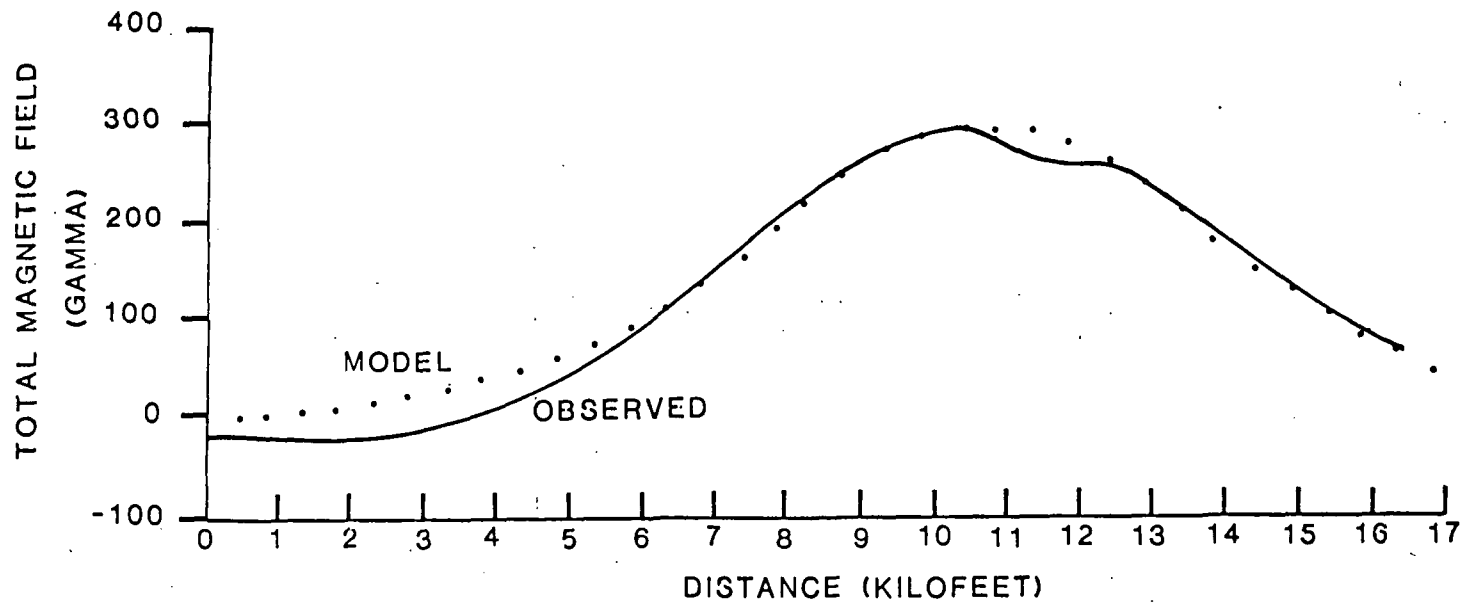


FIGURE 30. TOTAL MAGNETIC FIELD, MODEL AND OBSERVED, LINE 5.

VII. CONCLUSIONS

The usefulness of seismic methods for delineation of geologic structure in a porphyry copper prospect has been demonstrated. The reflection seismic sections delineate a regional westward dipping structure with a localized shear stress pattern resulting from forceful injections of intrusive material from below. Three of the numerous faults have surface traces that have not been previously detected in the fifteen years of exploration by most other geophysical exploration methods. These faults traverse all lithologic units including a recent active fanglomerate indicating continued tectonic activity up to the present. In several places an echelon faulting has produced replication of lithologic units that was not identified in the drill holes.

A high grade of metamorphism apparently has prevailed throughout much of the prospect. The undisturbed beds in the central valley have excellent reflections and clear separations. Within the disturbed zone, the reflections are much less distinct because of the extensive alteration. With careful interpretation, much of the faulting can be identified and the lithology can be interpreted in the immediate vicinity of the drill holes. Additional development is necessary to identify lithologic units solely from the reflection sections.

There is no identification of the concentric alteration-mineralization zones as depicted in the model of Lowell and Guilbert (1970). However, many of the structural features described by James (1976) in the Robinson mining district are prevalent in the seismic sections. These main features are: contact metamorphism along fault contacts between intrusive bodies and host rocks; many small, closely spaced, parallel faults; frequently occurring fault gouge; distorted beds; and high grade metamorphism that complicates relict bed identification.

The refraction data were used to identify six layers with a complicated geological structure, to identify several major faults with offsets of 75 to 300 m, to detect layers having velocities of 6300 m/s representative of competent igneous rocks, and to define a small area of high velocity rocks about 610 m ESE of drill hole BV9. Refraction data can supplement reflection data for generalized lithologic interpretations. However, refraction data should not be used alone for developing an exploratory drill hole program.

The application of reflection data to obtain realistic models for the interpretation of magnetic data has been illustrated.

VIII. RECOMMENDATIONS

It is recommended that seismic reflection surveys should be considered as a necessary prospect evaluation technique that precedes and later supplements the exploratory drilling program. This recommendation is based on the cost effectiveness of requiring fewer drill holes to establish the existence of an economical ore body. It is further recommended that concurrent with the reflection survey, that refraction seismic data be collected as a first evaluation of the lithologic units within the structure determined from the reflection data.

The structure of a porphyry mineral deposit can be determined adequately, but lithologic detection of the altered rocks needs development. It is recommended that a low level, auxiliary program be established to improve this capability. The first objective of this program would be to collect data on elastic properties of rock assemblages common to porphyry deposits. As an essential part of this objective, it is recommended that sonic and density logs be made in all holes GMRC drills in porphyry deposits. It is also recommended that samples of cores of all rock types encountered be tested at a commercial laboratory or at a university for P-wave and S-wave velocities and density as a function of near surface pressures

and temperatures. As data from the literature and these tests are accumulated, the seismic response of porphyry rocks can be modelled and compared to surveys that are available. Lithologic detection is a goal worthy of pursuing, but the data obtained in this survey do not justify a major effort at this time. When hard numbers are available on elastic properties of specific rocks and on elastic contrasts between rocks, the potential success of lithologic detection can be better evaluated.

It is recommended that future R & D experiments evaluate methods of performance/cost tradeoffs. Better resolution of thinner beds can be obtained with higher frequencies, by summing of repetitive shots, and by changes in the detection system parameters. Lower costs can be achieved with surface sources and single detectors per station rather than geophone arrays.

James E. Fix

J. E. Fix

Approved

J. A. Kehey for DTT

Date

Distribution
Approved

Hall

Date

July 29, 76

JEF/smh

References

- Armstrong, Richard Lee, 1972, Low Angle (denudation) Faults, Hinterland of the Sevier Orogenic Belt, Eastern Nevada and Western Utah: Geol. Soc. Amer. Bull., v. 83, p. 1729-1754.
- Collinson, James W. Christopher G. St. C. Kendall, and Jonathan B. Marcantel, 1976, Permian-Triassic Boundary in Eastern Nevada and West-Central Utah: Geol. Soc. Amer. Bull., v. 87, p. 821-824.
- Frangos, W. and P. M. Wright, 1972, Butte Valley-Cyprus Examination, White Pine County, Nevada, Geophysical Results: Kennecott Exploration, Inc. (KEI) Report.
- Fritz, William H., 1968, Geologic Map and Sections of the Southern Cherry Creek and Northern Egan Ranges, White Pine County, Nevada: Nevada Bur. Mines Map No. 35, Mackay School of Mines, Univ. Nevada.
- James, Lawrence P., 1976, Zoned Alteration in Limestone at Porphyry Copper Deposits, Ely, Nevada: Economic Geol., v. 71, p. 488-512.
- Lowell, J. David and John M. Guilbert, 1970, Lateral and Vertical Alteration-Mineralization Zoning in Porphyry Ore Deposits: Economic Geol., v. 65, no. 4, p. 373-408.
- Marcantel, Jonathan, 1975, Late Pennsylvanian and Early Permian Sedimentation in Northeast Nevada: Amer. Assoc. Pet. Geol. Bull., v. 59, no. 11, p. 2079-2098.
- Miller, Robert D., 1971, 1971 Progress Report Butte Valley - Cyprus Examination: Bear Creek Mining Company Report.
- Scott, James H., Benton L. Tibbetts, and Richard G. Burdick, 1970, Computer Analysis of Seismic Refraction Data, Report of Investigation 7595: Bur. of Mines, U. S. Dept. of Interior, 95 p.
- Welsh, John E., 1967, Geology of the Southwest Side, South Cherry Creek Mountains, Butte Valley: Bear Creek Mining Co., Geologic Map, September.
- Welsh, John E., Sept. 21, 1972a, Memo to Files; Subject: Interpretation of DDH BV-5, Butte Valley Project, T22N, R61E, White Pine County, Nevada: Kennecott Exploration, Inc.
- Welsh, John E., Sept. 21, 1972b, Memo to Files; Subject: Skarn Interpretation, DDH BV-2, Butte Valley Project, T22N, R61E, White Pine County, Nevada: Kennecott Exploration, Inc.
- Welsh, John E., February 17, 1976, Memo to P. M. Wright, Subject: Subsurface Data in Butte Valley Project Area, White Pine County, Nevada (Data for Seismic Interpretation): Kennecott Exploration, Inc.

Acknowledgements

The author would like to acknowledge the support given to this project by others at GS&TC. Mark Kramer performed most of the data processing of the reflection sections. The data were collected by the GS&TC research crew: Robert G. Slater, Party Chief; Alan L. Cogley, Research Technician; and Justin R. Decheck, Research Technician. The field program was planned by R. L. Geyer, Research Associate and J. A. McDonald, Research Geophysicist. P. G. Mathieu, Department Manager, assisted in establishing field data collection parameters.